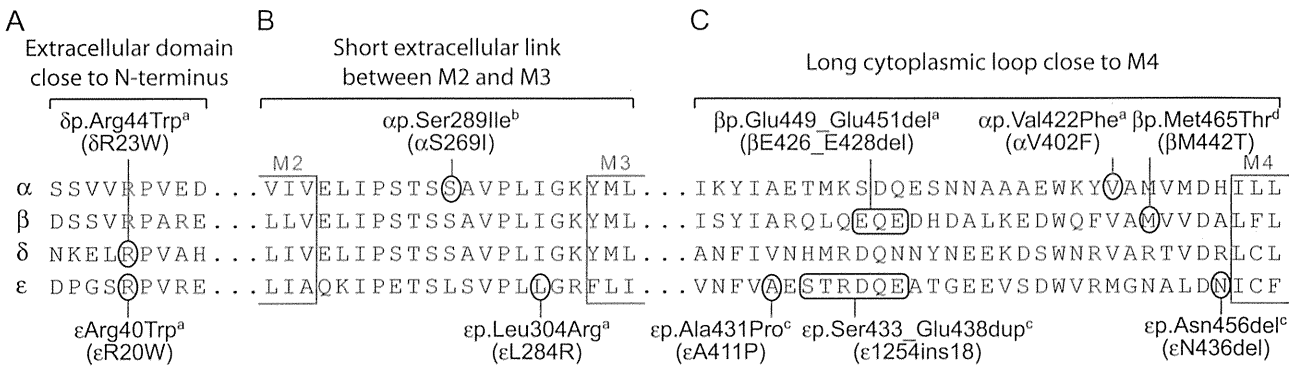

Fig. 5. Positions of the currently identified δp.Arg44Trp, εp.Leu304Arg and βp.Met465Thr, as well as previously reported CMS mutations. Mutations in the extracellular domain close the N-terminal end (A), the short extracellular link between the M2 and M3 transmembrane domains (B), and the long cytoplasmic loop close to the M4 transmembrane domain (C) are indicated. [a]δp.Arg44Trp (current report), εp.Arg40Trp [35], βp.Glu449_Glu451del [36], and αp.Val422Phe [37] cause AChR deficiency (AChR def.). [b]αp.Ser289Ile [38] causes SCCMS. [c]εp.Ala431Pro [24], ε p.Ser433_Glu438dup [23], and εp.Asn456del [34] cause FCCMS. [d]βp.Met465Thr is a currently analyzed polymorphism that shortens channel opening events. Mutations in parentheses are legacy annotations used in the original reports.

mutation in this region, εp.Asn456del (εN436del), destabilizes the diliganded receptor [34]. The C-terminal region of the long cytoplasmic loop of the ε subunit is thus likely to be crucial for stabilizing the open channel. In contrast to the three FCCMS mutations in the C-terminal end, however, βp.Met465Thr mildly shortens channel opening events and has no effect on the fidelity of channel gating, which may represent subunit-specificity and/or position-specificity of the amino acid substitutions.

Excluding δp.Arg44Trp that was previously reported in a healthy subject of unknown ethnicity [17], five of the six mutations in the AChR subunit genes in the current study and the five previously identified *COLQ* mutations [8] are unique to Japanese people. This is in contrast to some CMS mutations that are observed in unrelated families in Western and Middle Eastern countries. Especially, founder effects are implicated in two mutations: p.Asn88Lys in *RAPSN* [9–11] and c.1124_1127dupTGCC in *DOK7* [12]. CMS mutations are all recessively inherited except for those causing SCCMS. As heterozygous carriers of recessive CMS mutations exhibit no clinical phenotypes even by detailed electrophysiological studies, an asymptomatic carrier of a recessive CMS mutation has no disadvantage in transmitting the mutant allele to offspring. Lack of founder effects between the Japanese patients and patients of other nationalities thus suggest that most but not all CMS mutations arose *de novo* in a recent human history or in each family.

Acknowledgments

This study was supported by Grants-in-Aid from the MEXT and MHLW of Japan to KO. We would like to thank Dr. Andrew G. Engel for critical and constructive discussion on this project.

References

[1] Borges LS, Yechikhov S, Lee YI, et al. Identification of a motif in the acetylcholine receptor beta subunit whose phosphorylation regulates rapsyn association and postsynaptic receptor localization. J Neurosci 2008;28:11468–76.
[2] Bezakova G, Ruegg MA. New insights into the roles of agrin. Nat Rev Mol Cell Biol 2003;4:295–308.
[3] Budnik V, Salinas PC. Wnt signaling during synaptic development and plasticity. Curr Opin Neurobiol 2011;21:151–9.
[4] Korkut C, Budnik V. WNTs tune up the neuromuscular junction. Nat Rev Neurosci 2009;10:627–34.
[5] Ohno K, Ito M, Engel AG. Congenital myasthenic syndromes – molecular bases of congenital defects of proteins at the neuromuscular junction. In: Zaher A, editor. Neuromuscul. Disord. Rijeka: InTech; 2012. p. 175–200.
[6] Croxen R, Hatton C, Shelley C, et al. Recessive inheritance and variable penetrance of slow-channel congenital myasthenic syndromes. Neurology 2002;59:162–8.
[7] Ohno K, Engel AG, Brengman JM, et al. The spectrum of mutations causing endplate acetylcholinesterase deficiency. Ann Neurol 2000;47:162–70.
[8] Nakata T, Ito M, Azuma Y, et al. Mutations in the C-terminal domain of ColQ in endplate acetylcholinesterase deficiency compromise ColQ-MuSK interaction. Hum Mutat 2013;34:997–1004.
[9] Ohno K, Engel AG. Lack of founder haplotype for the rapsyn N88K mutation: N88K is an ancient founder mutation or arises from multiple founders. J Med Genet 2004;41:e8.
[10] Muller JS, Abicht A, Burke G, et al. The congenital myasthenic syndrome mutation RAPSN N88K derives from an ancient Indo-European founder. J Med Genet 2004;41:e104.
[11] Dunne V, Maselli RA. Common founder effect of rapsyn N88K studied using intragenic markers. J Hum Genet 2004;49:366–9.
[12] Ben Ammar A, Petit F, Alexandri N, et al. Phenotype genotype analysis in 15 patients presenting a congenital myasthenic syndrome due to mutations in DOK7. J Neurol 2010;257:754–66.
[13] Ohno K, Wang HL, Milone M, et al. Congenital myasthenic syndrome caused by decreased agonist binding affinity due to a mutation in the acetylcholine receptor epsilon subunit. Neuron 1996;17:157–70.
[14] Shen XM, Fukuda T, Ohno K, Sine SM, Engel AG. Congenital myasthenia-related AChR delta subunit mutation interferes with intersubunit communication essential for channel gating. J Clin Invest 2008;118:1867–76.
[15] Ishigaki K, Murakami T, Ito Y, et al. [Treatment approach to congenital myasthenic syndrome in a patient with acetylcholine receptor deficiency]. No to Hattatsu 2009;41:37–42.
[16] Irahara K, Komaki H, Honda R, et al. [Clinical features of congenital myasthenic syndrome in Japan]. No to Hattatsu 2012;44:450–4.
[17] Denning L, Anderson JA, Davis R, Gregg JP, Kuzdenyi J, Maselli RA. High throughput genetic analysis of congenital myasthenic syndromes using resequencing microarrays. PLoS ONE 2007;2:e918.

[18] Narahara M, Higasa K, Nakamura S, et al. Large-scale East-Asian eQTL mapping reveals novel candidate genes for LD mapping and the genomic landscape of transcriptional effects of sequence variants. PLoS ONE 2014;9:e100924.
[19] Engel AG, Ohno K, Bouzat C, Sine SM, Griggs RC. End-plate acetylcholine receptor deficiency due to nonsense mutations in the epsilon subunit. Ann Neurol 1996;40:810–17.
[20] Engel AG, Ohno K, Milone M, et al. New mutations in acetylcholine receptor subunit genes reveal heterogeneity in the slow-channel congenital myasthenic syndrome. Hum Mol Genet 1996;5:1217–27.
[21] Ohno K, Quiram PA, Milone M, et al. Congenital myasthenic syndromes due to heteroallelic nonsense/missense mutations in the acetylcholine receptor epsilon subunit gene: identification and functional characterization of six new mutations. Hum Mol Genet 1997;6:753–66.
[22] Ohno K, Hutchinson DO, Milone M, et al. Congenital myasthenic syndrome caused by prolonged acetylcholine receptor channel openings due to a mutation in the M2 domain of the epsilon subunit. Proc Natl Acad Sci U S A 1995;92:758–62.
[23] Milone M, Wang H-L, Ohno K, et al. Mode switching kinetics produced by a naturally occurring mutation in the cytoplasmic loop of the human acetylcholine receptor epsilon subunit. Neuron 1998;20:575–88.
[24] Wang H-L, Ohno K, Milone M, et al. Fundamental gating mechanism of nicotinic receptor channel revealed by mutation causing a congenital myasthenic syndrome. J Gen Physiol 2000;116:449–62.
[25] Shen X-M, Ohno K, Tsujino A, et al. Mutation causing severe myasthenia reveals functional asymmetry of AChR signature cystine loops in agonist binding and gating. J Clin Invest 2003;111:497–505.
[26] Shen XM, Brengman JM, Sine SM, Engel AG. Myasthenic syndrome AChRalpha C-loop mutant disrupts initiation of channel gating. J Clin Invest 2012;122:2613–21.
[27] Webster R, Brydson M, Croxen R, Newsom-Davis J, Vincent A, Beeson D. Mutation in the AChR ion channel gate underlies a fast channel congenital myasthenic syndrome. Neurology 2004;62:1090–6.
[28] Wang H-L, Milone M, Ohno K, et al. Acetylcholine receptor M3 domain: stereochemical and volume contributions to channel gating. Nat Neurosci 1999;2:226–33.
[29] Brownlow S, Webster R, Croxen R, et al. Acetylcholine receptor d subunit mutations underlie a fast-channel myasthenic syndrome and arthrogryposis multiplex congenita. J Clin Invest 2001;108:125–30.
[30] Shen XM, Ohno K, Fukudome T, et al. Congenital myasthenic syndrome caused by low-expressor fast-channel AChR delta subunit mutation. Neurology 2002;59:1881–8.
[31] Webster R, Liu WW, Chaouch A, Lochmuller H, Beeson D. Fast-channel congenital myasthenic syndrome with a novel acetylcholine receptor mutation at the alpha-epsilon subunit interface. Neuromuscul Disord 2014;24:143–7.
[32] Shen XM, Brengman JM, Edvardson S, Sine SM, Engel AG. Highly fatal fast-channel syndrome caused by AChR epsilon subunit mutation at the agonist binding site. Neurology 2012;79:449–54.
[33] Sine SM, Shen X-M, Wang H-L, et al. Naturally occurring mutations at the acetylcholine receptor binding site independently alter ACh binding and channel gating. J Gen Physiol 2002;120:483–96.
[34] Shen XM, Ohno K, Sine SM, Engel AG. Subunit-specific contribution to agonist binding and channel gating revealed by inherited mutation in muscle acetylcholine receptor M3-M4 linker. Brain 2005;128:345–55.
[35] Shen X-M, Ohno K, Milone M, Brengman JM, Spilsbury P, Engel AG Low-affinity fast-channel syndrome. Neurology 2001;56(Suppl. 3):A60. (abstract).
[36] Quiram PA, Ohno K, Milone M, et al. Mutation causing congenital myasthenia reveals acetylcholine receptor beta/delta subunit interaction essential for assembly. J Clin Invest 1999;104:1403–10.
[37] Milone M, Shen X-M, Ohno K, et al. Unusual congenital myasthenic syndrome with endplate AChR deficiency caused by alpha subunit mutations and a remitting-relapsing clinical course. Neurology 1999;51(Suppl. 2):A185. (abstract).
[38] Croxen R, Newland C, Beeson D, et al. Mutations in different functional domains of the human muscle acetylcholine receptor alpha subunit in patients with the slow-channel congenital myasthenic syndrome. Hum Mol Genet 1997;6:767–74.

Human Molecular Genetics, 2014, Vol. 23, No. 7 **1856–1868**
doi:10.1093/hmg/ddt578
Advance Access published on November 13, 2013

LRP4 third β-propeller domain mutations cause novel congenital myasthenia by compromising agrin-mediated MuSK signaling in a position-specific manner

Bisei Ohkawara[1], Macarena Cabrera-Serrano[3], Tomohiko Nakata[1], Margherita Milone[3], Nobuyuki Asai[1], Kenyu Ito[1], Mikako Ito[1], Akio Masuda[1], Yasutomo Ito[2], Andrew G. Engel[3,*] and Kinji Ohno[1,*]

[1]Division of Neurogenetics, Center for Neurological Diseases and Cancer and [2]Division for Medical Research Engineering, Nagoya University Graduate School of Medicine, Nagoya, Japan [3]Department of Neurology, Mayo Clinic, Rochester, MN, USA

Received June 10, 2013; Revised October 15, 2013; Accepted November 11, 2013

Congenital myasthenic syndromes (CMS) are heterogeneous disorders in which the safety margin of neuromuscular transmission is compromised by one or more specific mechanisms. Using Sanger and exome sequencing in a CMS patient, we identified two heteroallelic mutations, p.Glu1233Lys and p.Arg1277His, in *LRP4* coding for the postsynaptic low-density lipoprotein receptor-related protein 4. LRP4, expressed on the surface of the postsynaptic membrane of the neuromuscular junction, is a receptor for neurally secreted agrin, and LRP4 bound by agrin activates MuSK. Activated MuSK in concert with Dok-7 stimulates rapsyn to concentrate and anchor AChR on the postsynaptic membrane and interacts with other proteins implicated in the assembly and maintenance of the neuromuscular junction. LRP4 also functions as an inhibitor of Wnt/beta-catenin signaling. The identified mutations in *LRP4* are located at the edge of its 3rd beta-propeller domain and decrease binding affinity of LRP4 for both MuSK and agrin. Mutations in the LRP4 3rd beta-propeller domain were previously reported to impair Wnt signaling and cause bone diseases including Cenani–Lenz syndactyly syndrome and sclerosteosis-2. By analyzing naturally occurring and artificially introduced mutations in the LRP4 3rd beta-propeller domain, we show that the edge of the domain regulates the MuSK signaling whereas its central cavity governs Wnt signaling. We conclude that *LRP4* is a new CMS disease gene and that the 3rd beta propeller domain of LRP4 mediates the two signaling pathways in a position-specific manner.

INTRODUCTION

Congenital myasthenic syndromes (CMS) are diverse disorders in which the safety margin of neuromuscular transmission is compromised by deficiency or abnormal function of an endplate (EP)-associated protein. To date, mutations in no fewer than 17 genes coding for proteins expressed at EP are known to cause CMS (1): *ALG2* (MIM 607905), *ALG14* (MIM 612866), *CHRNA1* (MIM 100690), *CHRNB1* (MIM 100710), *CHRND* (MIM 100720), *CHRNE* (MIM 100725), *AGRN* (MIM 103320), *CHAT* (MIM 118491), *DPAGT1* (MIM 191350), *GFPT1* (MIM 138292), *LAMB2* (MIM 150325), *PLEC* (MIM 601282), *MUSK* (MIM 601296), *RAPSN* (MIM 601592), *COLQ* (MIM 603033), *SCN4A* (MIM 603967) and *DOK7* (MIM 610285). We here describe our findings in a novel CMS caused by mutations in the low-density lipoprotein receptor-related protein 4 encoded by *LRP4*.

EP development is triggered by the binding of agrin released from the nerve terminal to LRP4, a transmembrane protein of the

*To whom correspondence should be addressed at: Division of Neurogenetics, Center for Neurological Diseases and Cancer, Nagoya University Graduate School of Medicine, 65 Tsurumai, Showa-ku, Nagoya, Aichi 466-8550, Japan. Tel: +81 52 744 2446; Fax: +81 52 744 2449; Email: ohnok@med.nagoya-u.ac.jp (K.O.); Neuromuscular Research Laboratory, Department of Neurology, Mayo Clinic, 200 First Street SW, Rochester, MN 55905, USA. Tel: +1 507 284 5102; Fax: +1 507 2845831; Email: age@mayo.edu (A.G.E.)

postsynaptic membrane (2,3). LRP4 bound to agrin forms a ternary complex with the postsynaptic transmembrane muscle-specific receptor tyrosine kinase (MuSK). In this complex, the 3rd β-propeller domain of LRP4 is important for association with MuSK (4), although the interacting conformations remain unresolved. Binding of LRP4 to MuSK triggers phosphorylation and activation of the MuSK intracellular kinase domain. Activated MuSK in concert with Dok-7 stimulates rapsyn to concentrate and anchor AChR in the postsynaptic membrane and to interact with other proteins implicated in the assembly and maintenance of the NMJ (5). LRP4 was recently reported to provide a retrograde signal for presynaptic differentiation at neuromuscular junction (6,7). In addition, autoantibodies directed against LRP4 were recently recognized to cause a form of autoimmune myasthenia gravis (8–10).

In addition to its specific role at the NMJ, LRP4 is also a well-characterized inhibitor of the Wnt-signaling pathway. LRP4 signaling is involved in skeleton formation and kidney development. Mutations in *LRP4* have been reported in Cenani–Lenz syndactyly syndrome (CLSS) (11), sclerosteosis-2 (12), and low bone mineral density in human (13) and mice (14). Similarly, *Lrp4* mutations cause mule foot disease in cow (15) and kidney and limb defects in mouse (16). In addition, a missense SNP rs2306029 in *LRP4* is associated with 4.17-fold increase in the risk of developing Richter syndrome (17). To date, no report has implicated *LRP4* as a CMS disease gene.

Using Sanger and exome-capture resequencing, we identified two heteroallelic missense variants in *LRP4*, p.Glu1233Lys (c.3697G > A) and p.Arg1277His (c.3830G > A). Both variants are located at the edge of the 3rd β-propeller domain of LRP4. We show that each variant impairs binding ability of LRP4 for both agrin and MuSK as well as subsequent agrin-mediated phosphorylation and activation of MuSK, but neither mutation affects the Wnt-signaling pathway. Finally, by analysis of mutations in other diseases and by examining effects of artificially engineered mutations into the 3rd LRP4 β-propeller domain, we show the edge of this domain mediates the MuSK signaling, whereas its central cavity mediates the Wnt signaling.

RESULTS

Clinical data

The patient was born after 42 weeks of gestation with fetal distress and with Apgar scores of 3 and 6 at 1 and 5 min, respectively. Immediately after birth, she had a respiratory arrest and required hospitalization for feeding and respiratory support until the age of 6 months. She started to walk at 18 months but could only walk short distances. During childhood, she fatigued abnormally, could not climb step and was partially wheelchair dependent. Examination at the Mayo Clinic at ages 9 and 14 years revealed mild eyelid ptosis, slight limitation of lateral eye movements, moderately severe proximal greater than distal muscle weakness and hypoactive tendon reflexes. Repetitive nerve stimulation of the spinal accessory nerve showed a 13–16% decrement of the fourth compared with the first compound muscle action potential evoked from the trapezius, biceps and rectus femoris muscles with no significant decrement in the anterior tibial muscle. The decremental responses were transiently improved by edrophonium chloride, a fast acting cholinergic agonist. However, therapy for a few days with pyridostigmine at age 12 markedly worsened the patient's weakness. There was no history of similarly affected family members.

Endplate studies

An intercostal muscle specimen was obtained from the patient at age 17 years. Routine histologic examination revealed type 1 fiber preponderance. Synaptic contacts, examined in face-on views of glutaraldehyde-fixed AChE-reacted teased muscle fibers revealed multiple irregularly arrayed synaptic contacts that varied in shape and size (Fig. 1). None of the EPs had a normal pretzel shape. Electron microscopy examination of 54 EP regions of 29 EPs showed that the structural integrity of the nerve terminals and postsynaptic regions was preserved but quantitative analysis revealed that the size of the nerve terminals was reduced to 60%, and that of the postsynaptic region to 48%, of the corresponding control value (Table 1).

Immunofluorescence microscopy examination of frozen sections revealed normal expression of AChR and AChE at patient EPs. Ultrastructural localization of AChR at the EPs with peroxidase-labeled α-bungarotoxin (bgt) demonstrated normal distribution and density of AChR on the junctional folds. However, the total number of AChRs per EP fell slightly below the range of control values (Table 1).

The MEPP amplitude and the number of quanta released by nerve impulse fell in the normal range, and patch-clamp recordings from10 EPs revealed normal kinetics of the AChR channel (data not shown).

Sanger and exome-capture resequencing analysis

We analyzed the patient DNA using the exome-capture resequencing analysis. The number of SOLiD tags was 90.7×10^6

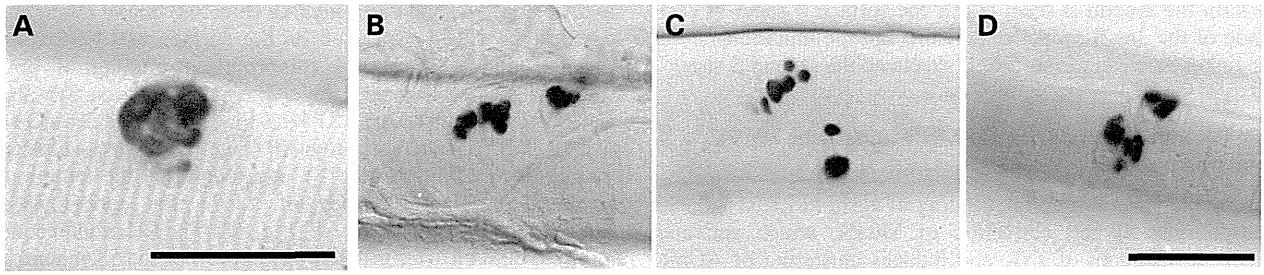

Figure 1. Synaptic contacts in intercostal muscle visualized by the cholinesterase reaction. (**A**) Normal EP. (**B–D**) Patient EPs. Note irregularly arrayed pleomorphic synaptic contacts at patient EPs. Bar in (A) indicates 50 μm. Bar in (D) indicates 50 μm for panels (B–D).

Table 1. Quantitative analysis of EP ultrastructure and [^{125}I]α-bungarotoxin-binding sites per EP

	Patient	Controls	*P*-value
Nerve terminal area (μm^2)	2.45 ± 0.30 (54)	3.88 ± 0.39 (63)	<0.005
Postsynaptic area (μm^2)	5.51 ± 0.45 (54)	10.6 ± 0.79 (59)	<0.001
[^{125}I]α-bgt-binding sites/EP	8.7×10^6	$12.82 \pm 0.79 \times 10^6$ (13) Range: 9.3–18.7	

Values represent mean ± SE. More than one region can occur at an EP. Values in parenthesis represent number of EP regions except for [^{125}I]α-bgt-binding sites where they indicate number of subjects. *P*-values are based on *t*-test.

spanning 4.53 Gb, and 72.8×10^6 tags (80.2%) spanning 3.47 Gb (76.6%) were mapped to the human genome hg19/GRCh37. As the SureSelect probes span 38 Mb, the mean coverage became 91.4. Among the 38-Mb SureSelect probe regions, 3.9% of nucleotides were not covered by any tags. Search for SNVs and indels using Avadis NGS with default parameters detected 46 555 SNVs/indels. We eliminated SNVs/indels registered in dbSNP137 and those with unreliable calls (Avadis decibel score ≤200), and obtained 4074 SNVs/indels. Restriction of our analysis to non-synonymous, frameshifting and splicing SNVs/indels in 33 candidate genes that are essential for the neuromuscular signal transmission yielded three SNVs. Among the three SNVs, a heterozygous c.1148C > G SNV predicting p.Ser376Arg in *SNTB2* encoding syntrophin β_2 was observed in a patient with periodic paralysis among our cohort of 31 patients other than CMS. In addition, 13 other missense SNPs and two frameshifting SNPs are registered in 539 codons encoded by *SNTB2* in dbSNP137. Thus, p.Ser376Arg in *SNTB2* was unlikely to be pathogenic. The two other SNVs were heterozygous c.3697G > A (chr11: 46 897 357) and c.3830G > A (chr11: 46 897 102) in *LRP4*, which predicted p.Glu1233Lys (EK mutation) and p.Arg1277His (RH mutation), respectively. Sanger sequencing of the patient's genomic DNA and mRNA confirmed both mutations and sequencing of cloned mRNA indicated that the mutations were heteroallelic. The father was heterozygous for p.Glu1233Lys. A half brother carried no mutation. No DNA was available from the mother. According to the PolyPhen-2 (18), SIFT (19) and Mutation Taster (20) algorithms, the predicted consequences of the EK mutation were 'benign', 'tolerated' and 'disease causing with $P > 0.99999$', respectively. Those of the RH mutation were 'probably damaging', 'affect protein function' and 'disease causing with $P > 0.99999$', respectively. LRP4 is a transmembrane protein with large extracellular domains (Fig. 2A). These mutations were in the 3rd low-density lipoprotein receptor (LDLR) type B repeat, known as β-propeller-like structure. The EK and RH mutations are downstream of the 4th and 5th YWTD motifs, respectively (Fig. 2B). The YWTD motifs are predicted to form the second β sheet below the surface β sheet of each blade of the 3rd β-propeller domain, and the mutations are at the linker between the surface β sheet and the second β sheet.

The EK and RH mutations in *LRP4* impair the MuSK signaling pathway

During the NMJ formation, binding of agrin to LRP4 induces phosphorylation and activation of MuSK, which activates ATF2 downstream of JNK and induces clustering of AChR. To study effects of the mutations in this signaling pathway, we used a JNK-responsive ATF2-luciferase (ATF2-luc) reporter (21), which specifically monitors MuSK-dependent stimulation in transfected HEK293 cells. Overexpression of LRP4 and MuSK activated the ATF2-luc reporter in the absence of agrin, as previously reported (22). The EK mutant minimally and the RH mutant moderately impaired LRP4-induced activation of ATF2-luc (Fig. 3A). Addition of agrin to the medium markedly enhanced the ATF2-luc activity for the wild-type LRP4, whereas both mutants completely abolished responsiveness to agrin (Fig. 3A).

We also examined effects of the mutations on MuSK phosphorylation that occurs immediately after formation of the agrin/LRP4/MuSK complex. Consistent with its effects on the signaling activity, agrin enhanced MuSK phosphorylation in the presence of wild-type LRP4 but not in the presence of mutant LRP4 in HEK293 cells (Fig. 3B) and in Lrp4-downregulated C2C12 myoblasts (Fig. 4B). Similarly, wild-type LRP4, but not EK and RH mutants, rescued AChR clustering in Lrp4-downregulated C2C12 myotubes (Fig. 4C). These results support the notion that the EK and RH mutations compromise agrin-mediated activation of MuSK and AChR clustering.

LRP4 has also been known as an extracellular antagonist for Wnt signaling. Wnt signaling is involved in tissue development including limb, bone and kidney. Indeed, previously reported mutations of *LRP4* in human, mouse and cow exhibit structural abnormalities in limb, bone and/or kidney. We thus examined the effects of our LRP4 mutations on Wnt-signaling pathway using the TOPFLASH reporter. Wild-type LRP4 suppressed the Wnt3a-mediated TOPFLASH activity, and the EK and RH mutations retained similar suppressive effects (Fig. 3C). Lack of limb, bone and kidney symptoms in our patient can be attributed to EK and RH only affecting agrin-induced activation of MuSK but having no effect on Wnt signaling.

LRP4 directly binds to agrin and MuSK through its extracellular domain. To test the effects of the LRP4 mutations on binding to MuSK and agrin, we performed cell surface-binding assays. We first confirmed that the EK and RH mutants had no effect on LRP4 expressions in cell body and cell membrane in COS7 cells (Supplementary Material, Fig. S1). MuSKect-mycAP (Fig. 5A) and agrin-mycAP (Fig. 5B) bound efficiently to wild-type LRP4 expressed on the surface of COS7 cells. The RH and EK mutants compromised binding of both MuSKect-mycAP and agrin-mycAP (Fig. 5A and B). We also analyzed direct binding of LRP4ecd-Flag to purified MuSKect-mycAP (Fig. 5C) and agrin-mycAP (Fig. 5D) by *in vitro* plate-binding assays (Fig. 5E and F). We found that the mutations decreased binding affinities of LRP4 for agrin-mycAP (Fig. 5E) and MuSKect-mycAP (Fig. 5F). The RH mutant compromised binding of agrin and MuSK more than the EK mutant in the cell surface-binding assay but not in the *in vitro* plate-binding assay, which may be accounted for by some other molecules

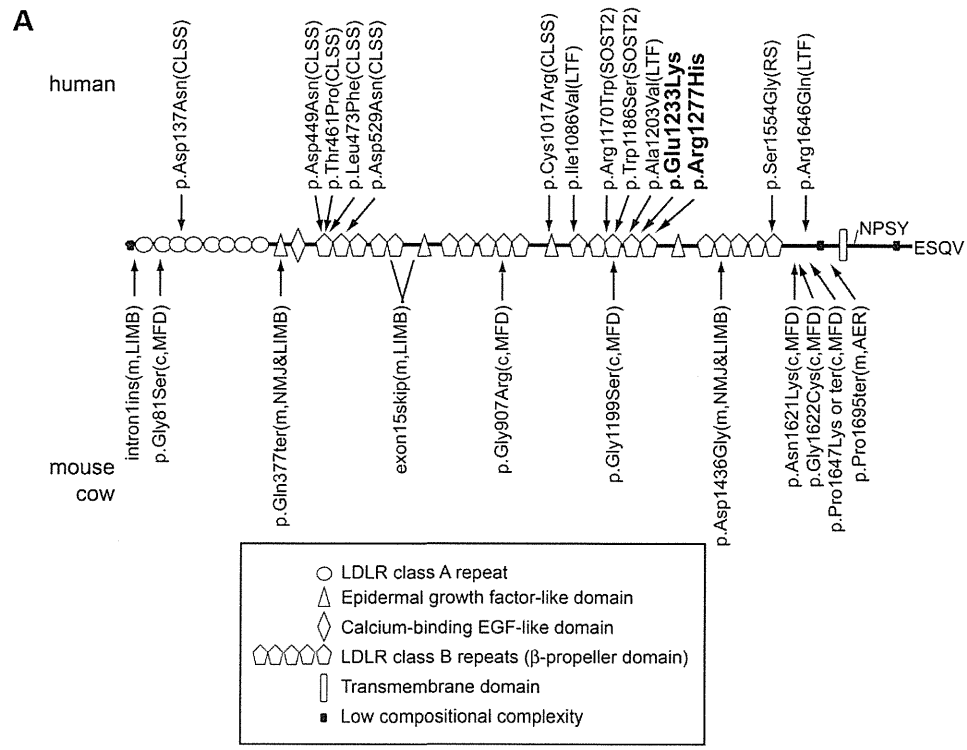

B

4th YWTD motif in 3rd LDLR type B repeat

p.Glu1233Lys

```
Homo sapiens.tx 1205 LINNNLGWPNGLTVDKASSQLLWADAHTERIEAADLNGANRHTLVSPVQHPYGLTLLDSY 1264
Bos taurus.txt  1205 LINSNLGWPNGLTVDKASSQLLWADAHTERIEAADLNGANRHTLVSPVQHPYGLTLLDAY 1264
Canis familiari 1321 LISNNLGWPNGLTVDKASSQLLWADAHTERIEAADLNGGSRHTLVSPVQHPYGLTLLDSY 1380
Rattus norvegic 1205 LINNNLGWPNGLTVDKTSSQLLWADAHTERIEVADLNGANRHTLVSPVQHPYGLTLLDSY 1264
Mus musculus.tx 1205 LINNNLGWPNGLTVDKTSSQLLWADAHTERIEVADLNGANRHTLVSPVQHPYGLTLLDSY 1264
Gallus gallus.t 1249 LISNNLGWPNGLAVDKAGSQLLWADAHTERIEAADLNGANRRTLLSPVQHPYGLTLLDSY 1308
Tetraodon nigro 1025 LISNNLGWPNGLAIDTAGSQLLWADAHTERIEAADLNGQNRRTLVTPVQHPYGLTLLGSH 1084
Drosophila mela 1381 IVTANLGWPNGLSLDLKSKRIYWVDARLKTIDSCDYTGNQRKLIMSSLHHPYALALSDDN 1440
Aedes aegypti.t 1422 IVTTDLGFVSGLAVDSVENRIYWTDSKAKRIESCDFNGNSRKILLNNLSHPYALTVTTST 1481
                      ..   **   **..*    .. * *..   *. .* .*  *. ..  . *** *..
```

5th YWTD motif in 3rd LDLR type B repeat

p.Arg1277His

```
Homo sapiens.tx 1265 IYWTDWQTRSIHRADKGTGSNVILVRSNLPGLMDMQAVDRAQP--LGFNKCGSRNGGCSH 1322
Bos taurus.txt  1265 IYWTDWQTRSIHRADKGTGSNVILVRSNLPGLMDIQAVDRSQP--LGVNKCGPRNGGCSH 1322
Canis familiari 1381 IYWTDWQTRSIHRADKGTGSNVILVRSNLPGLMDIQAVDRAQP--LGFNKCGSRNGGCSH 1438
Rattus norvegic 1265 IYWTDWQTRSIHRADKSTGSNVILVRSNLPGLMDIQAVDRAQP--LGFNKCGSRNGGCSH 1322
Mus musculus.tx 1265 IYWTDWQTRSIHRADKSTGSNVILVRSNLPGLMDIQAVDRAQP--LGFNKCGSRNGGCSH 1322
Gallus gallus.t 1309 IYWTDWQTRSIHRADKDSGANVILVRANLPGLMDIQAVDRARP--LGFNKCGVRNGGCSH 1366
Tetraodon nigro 1085 IYWTDWQSRSIQRADKTTGTNTITVRSNLPGLMDIQAVDMERP--LGFNKCGRRNGGCTH 1142
Drosophila mela 1441 IYWTDWKSKALHMTERRNISAKRDIITNIDGLMDIKIIYQNQNQSTMKNACGNNNGNCSH 1500
Aedes aegypti.t 1482 VYWTDWVTKALHSVSKLNTSKVRKVAKDLEELMDVKVVLGPSD--SQDDFCGKNNGGCSH 1539
                     .***** .....  .  .  .  .  ***.. .          **  **.*.*
```

Figure 2. Structure and previously identified mutations of LRP4. (**A**) Domain structure of LRP4 and positions of reported mutations in human, mouse and cow. p.Glu1233Lys (EK mutation) and p.Arg1277His (RH mutation) in the current studies are shown in bold. In human, LRP4 mutations cause CLSS (MIM 212780) and sclerosteosis-2 (SOST2, MIM 614305). SNPs are also associated with an increased risk for Richter syndromes (RS) and a low-trauma fracture (LTF) due to decreased bone mineral density. In mouse, mutations cause abnormal development of the apical ectodermal ridge (AER) leading to polysyndactyly and tooth abnormality, as well as abnormal developments of limbs (LIMB) and the neuromuscular junctions (NMJ). In cow, mutations lead to mulefoot disease (MFD). LRP4 harbors eight low-density lipoprotein receptor (LDLR) domain class A, four epidermal growth factor-like domains, a calcium-binding EGF-like domain, four LDLR class B repeat (β-propeller domain), a transmembrane domain and an intracellular domain. The LDLR type B repeat contains five tandem repeats of an YWTD motif to build a propeller-like structure. NPSY close to the C-terminal end is a motif for endocytosis and ESQV at the C-terminal end is a motif for binding to PDZ-containing proteins. (**B**) Positions of the EK and RH mutations downstream of the 4th and 5th YWTD motifs (boxed). The amino acid sequences are highly conserved across vertebrates but not in insects. Asterisks indicate strictly conserved amino acids, and dots indicate loosely conserved amino acids.

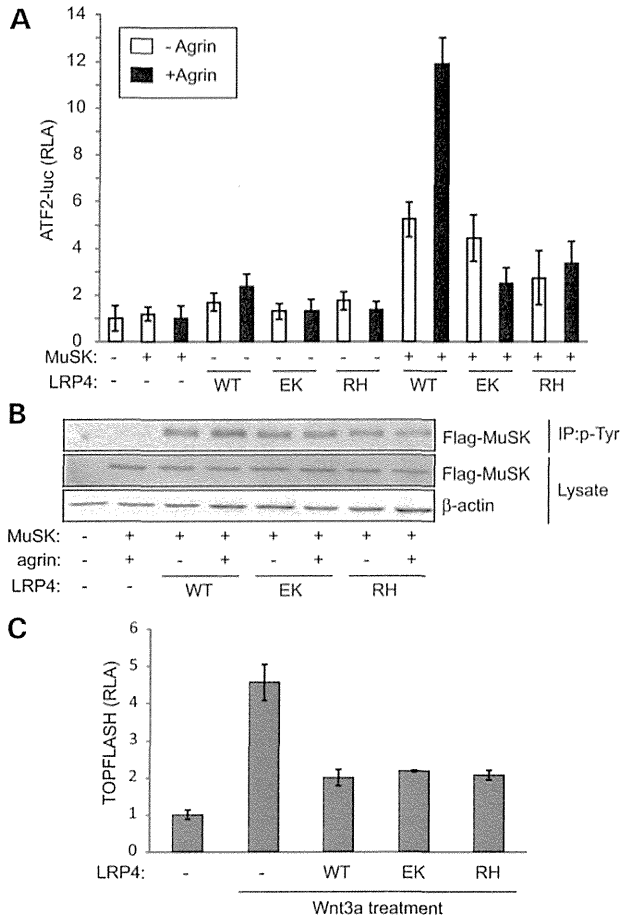

Figure 3. p.Glu1233Lys (EK) and p.Arg1277His (RH) mutants compromise agrin-mediated upregulation of MuSK signaling but retain Wnt-suppressive activity in HEK293 cells. (**A**) ATF2-luciferase reporter assay of HEK293 cells to quantify agrin-mediated activation of the MuSK signaling pathway. Cells were transfected with ATF2-luc reporter and Renilla reporter plasmids along with MuSK cDNA and the indicated LRP4 cDNA. Cells were cultured with or without 10 ng/μl agrin. Wild-type (WT) LRP4-activated MuSK without agrin, and agrin further enhanced the activation. The EK and RH mutations compromise MuSK activation in the presence or absence of agrin. (**B**) MuSK phosphorylation assay of HEK293 cells transfected with Flag-MuSK and the indicated *LRP4* cDNA with or without agrin (10 ng/μl). Phosphorylated MuSK was detected by immunoprecipitation of cell lysate by anti-phosphotyrosine antibody (p-Tyr) followed by immunoblotting with anti-FLAG antibody. Wild-type LRP4 phosphorylates MuSK, which is further enhanced by agrin, but EK and RH mutants abolish responsiveness to agrin. (**C**) TOPFLASH reporter assay of HEK293 cells to quantify responsiveness to Wnt3a. Cells were transfected with the TOPFLASH reporter and Renilla reporter plasmids along with the indicated *LRP4* cDNA. Cells were cultured in the presence or absence of Wnt3a. Means and SD are indicated. Wild-type (WT) and mutant LRP4 (EK and RH) suppress the Wnt3a-mediated signaling to the same extent.

expressed on the cell surface, beneath the cell membrane or secreted from the cells.

Mutations in *LRP4* causing sclerosteosis-2 have No effect on MuSK signaling

In contrast to our EK and RH mutations in the 3rd β-propeller domain, p.Arg1170Trp (abbreviated as RW) and p.Trp1186Ser (WS) mutations identified in a patient with sclerosteosis-2 impair Wnt-suppressing activity of LRP4 (12). We first confirmed that wild-type LRP4 and the two mutants are similarly expressed on the plasma membrane in HEK293 cells (Fig. 6A) as we observed in COS7 cells (Supplementary Material, Fig. S1). We then analyzed the effects of the two mutations on MuSK (Fig. 6B) and Wnt (Fig. 5C) signaling. Consistent with the previous report (12), the RW and WS mutations abrogated the Wnt-suppressing activity of LRP4 (Fig. 6C) but had no effect on agrin-induced MuSK signaling (Fig. 6B). Cell surface-binding assay also confirmed that the two mutants retained their ability to bind to agrin and MuSK (Fig. 6D).

As the four mutations affecting MuSK or Wnt signaling were all in the 3rd β-propeller domain, we scrutinized the positions of mutations by homology modeling of the 3rd β-propeller domain of human LRP4 using the 1st β-propeller domain of human LRP6 (PDB ID: 3SOV). The 3rd β-propeller domain contains six blade-like structures and displays a YWTD motif at the second β sheet below the surface of each blade (Fig. 7A and Supplementary Material, Movie S1). In this model, the EK and RH mutations, which only affect agrin/LRP4/MuSK signaling, are located on edge of the 5th and 6th blades, respectively (Fig. 7B and Supplementary Material, Movie S1). In contrast, the RW and WS mutations, which only affect Wnt signaling, are located in a central cavity of the propeller (Fig. 7C and Supplementary Material, Movie S1).

Artificially engineered Lrp4 mutations at the edge of the 3rd β-propeller domain affect MuSK signaling and those in the central cavity affect Wnt signaling

To further confirm that the edge of the 3rd β-propeller domain mediates MuSK signaling and that the central cavity mediates Wnt signaling, we introduced four other artificial mutations based on structural modeling of the 3rd β-propeller domain (Fig. 7A and Supplementary Material, Movie S1). As RH and EK mutations affected two exposed amino acids on the 2nd β sheet, we introduced an alanine into two neighboring amino acids to make IA and VA mutations (Fig. 7B and Supplementary Material, Movie S1). Similarly, as WS and RW mutations were facing the central cavity of the 3rd β-propeller domain, we introduced an alanine into the corresponding amino acids in the other blades to make YA and NA mutations (Fig. 7C and Supplementary Material, Movie S1). We then examined the effects of each mutation on MuSK and Wnt signaling. As expected, the VA and IA mutations at the edge of the 3rd β-propeller domain affected MuSK signaling (Fig. 8A), but not Wnt signaling (Fig. 8B). In contrast, the NA and YA mutations in the central cavity normally activated MuSK signaling (Fig. 8A), but lost Wnt-suppressive activity (Fig. 8B). Similarly, the cell surface-binding assay showed that the VA and IA mutations reduced binding of agrin and MuSK (Fig. 8C and D). Thus, the artificial mutations further underscore the differential signaling roles of the edge and the central cavity of the 3rd β-propeller domain.

DISCUSSION

LRP4 mutations cause a novel CMS

Because mutations in *AGRN* (25) and *MUSK* (26) have been known to cause CMS and because LRP4 was shown to be a

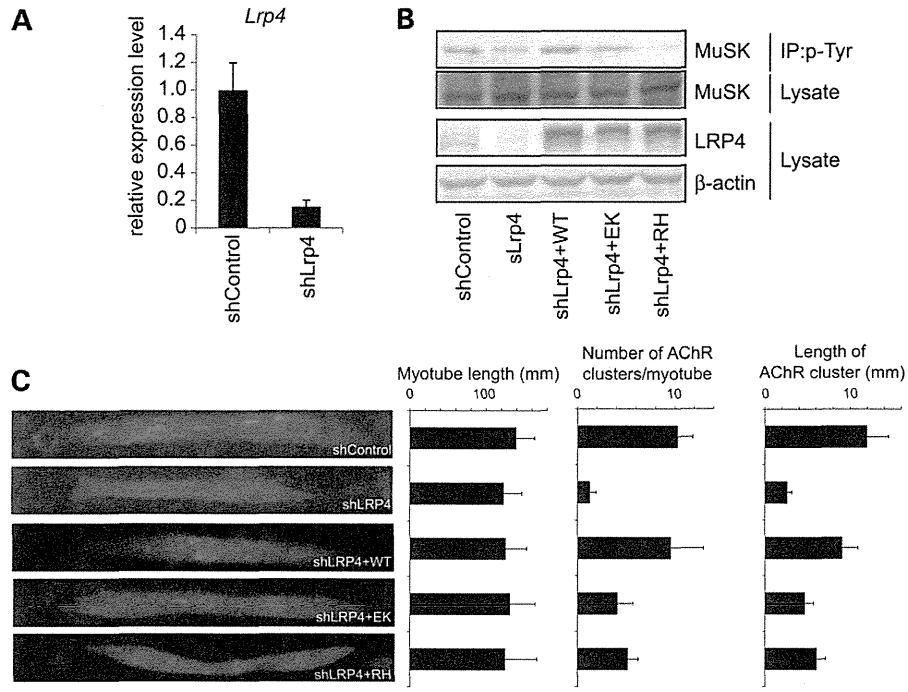

Figure 4. p.Glu1233Lys (EK) and p.Arg1277His (RH) mutants compromise agrin-mediated upregulation of MuSK signaling and AChR clustering in C2C12 myoblasts/myotubes. (**A**) Endogenous Lrp4 expression in C2C12 myoblasts is suppressed by shRNA against mouse Lrp4 (shLrp4) by qRT-PCR. (**B**) MuSK phosphorylation assay of differentiation-induced C2C12 myoblasts transfected with shControl or shLrp4 and the indicated *LRP4* cDNA. Phosphorylated MuSK was detected by immunoprecipitation of cell lysate by anti-phosphotyrosine antibody (p-Tyr) followed by immunoblotting with anti-MuSK antibody. Wild-type LRP4, but not EK and RH mutants, phosphorylates MuSK in Lrp4-deficient myoblasts. (**C**) Agrin-mediated AChR clustering in C2C12 myotubes. Myotubes are transfected with EGFP cDNA, shLRP4 and the indicated *LRP4* cDNA using electroporation. AChR is visualized with Alexa594-conjugated α-bungarotoxin at 12 h after adding 10 ng/ml agrin. Right panels: Morphometric analysis showing that wild-type (WT) LRP4, but not EK and RH mutants, rescues the number and the length of AChR clusters in Lrp4-downregulated C2C12 myotubes. LRP4 has no effect on myotube length.

coreceptor for agrin that mediates activation of MuSK (Fig. 7D) (2,3). *LRP4* has been a candidate gene for a CMS for a number of years. In this communication, we show that mutations in *LRP4* cause a CMS and that the identified mutations affect MuSK signaling by compromising binding of LRP4 to both agrin and MuSK.

Our data predict that the identified *LRP4* mutations interfere with agrin-LRP4-MusK signaling and thereby hinder concentration of AChR on the junctional folds as well as normal development and maintenance of the entire junction. Our EP studies show that the synaptic contacts are dysplastic (Fig. 1) and that the nerve terminal and postsynaptic areas at the EP regions are hypoplastic (Table 1), but the AChR content of EPs and the synaptic response to ACh are not appreciably reduced. Because the patient has a myasthenic disorders by clinical and EMG criteria, we attribute sparing of the intercostal muscles to different expressivity of the genetic defect in different muscles. Sparing of selected muscles can occur in both autoimmune and congenital myasthenias and is indicated by absence of muscle weakness or a decremental EMG response from some muscles in either disorder. For example, in MuSK antibody-positive myasthenia, EPs in intercostal and biceps brachii muscles have a normal AChR content, generate normal MEPP amplitudes, and have well preserved junctional folds (27,28). Analysis of *Musk* and *Lrp4* expressions in mouse muscles by quantitative RT–PCR revealed that expressions of *Musk* in omohyoid and trapezius muscles were less than those in the other muscles (Supplementary Material, Fig. S2). The least expression of *Musk* in mouse omohyoid has been recently reported (29). In contrast, *Musk* expression in intercostal muscle was ~three times more compared with omohyoid. Although human specimens of various muscles were not available for our studies, high and low MuSK expressions in intercostal and trapezius muscles may partly account for spared and impaired NMJ signal transmissions in intercostal and trapezius muscles, respectively, in our patient with *LRP4* mutations.

Position-specific disease phenotypes of *LRP4* mutations

The extracellular domain of LRP4 is known to bind to several proteins: agrin (2,3), MuSK (4), Wnt ligands (30), dkk1 (31), a Wnt inhibitor (32,33), sclerostin (31), another Wnt inhibitor (32,33) and possibly apoE (34). Specific binding domains of LRP4 have been dissected: agrin binds to the LDLa repeats 6–8, EGF-like domains, and the 1st β-propeller domain (Fig. 7B and Supplementary Material, Movie S1) (4,23); MuSK binds to the 4th/5th LDLa repeats and the 3rd β-propeller domain (4); sclerostin binds to the 3rd β-propeller domain (12); and apoE binds to LDLa (34). As for Wnt ligands, the precise molecular mechanisms how LRP4 suppresses Wnt signaling remain elusive, although the Wnt-suppressive effect of LRP4 is well established (35).

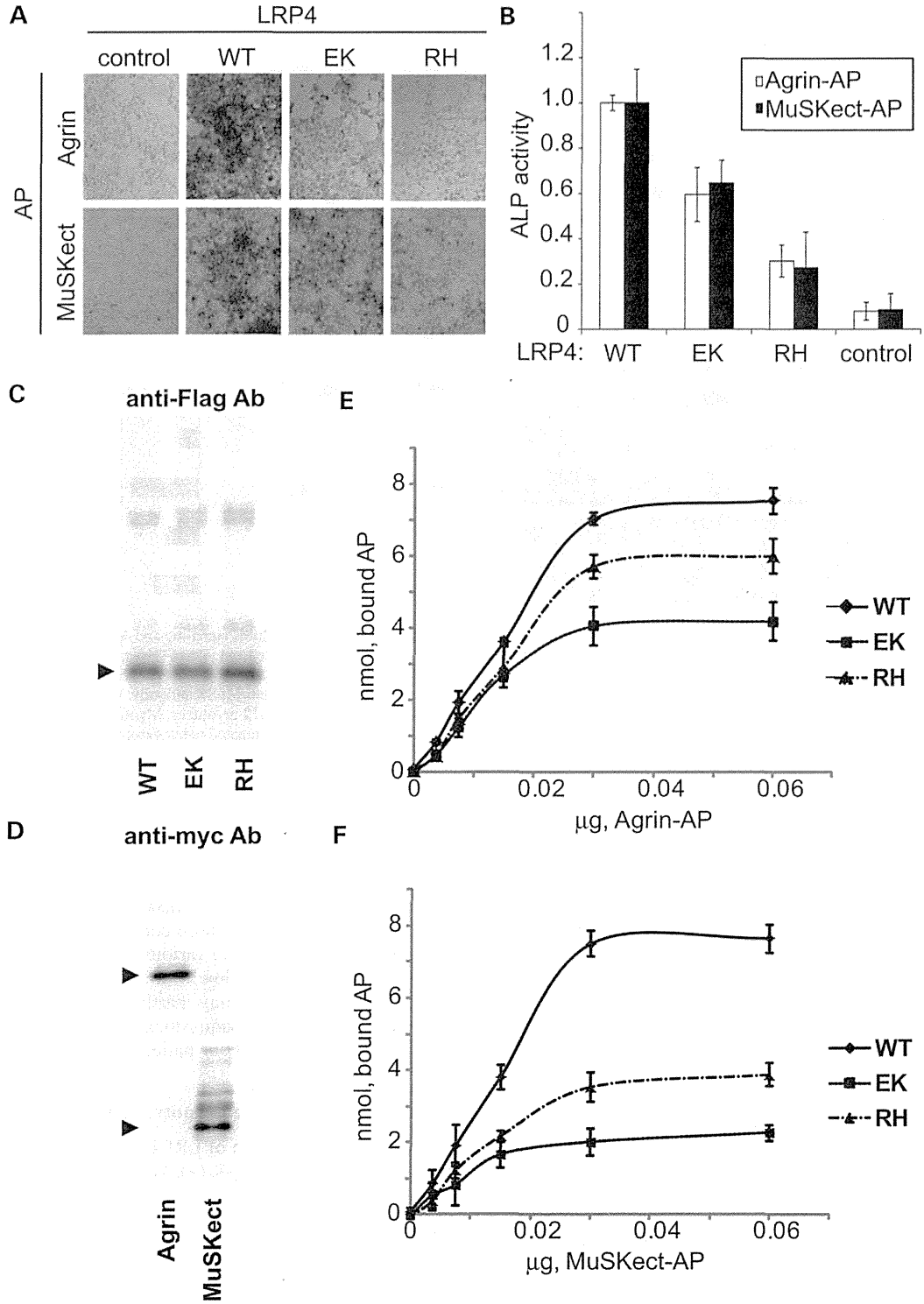

Figure 5. The p.Glu1233Lys (EK) and p.Arg1277His (RH) mutants impair binding of LRP4 to MuSK and agrin. (**A** and **B**) Cell surface-binding assays. COS7 cells were transfected with the wild-type or mutant *LRP4* cDNA and added with concentrated conditioned medium containing either neural Agrin-mycAP or MuSKect-mycAP as indicated. Control cells were transfected with an empty vector. Bound MuSKect-mycAP or agrin-mycAP was stained for the alkaline phosphatase activity (A). (B) The mean and SD of ALP activities of bound agrin-mycAP and MuSKect-mycAP in three independent wells. The RH and EK mutants reduce binding of MuSKect-mycAP and agrin-mycAP. (**C** and **D**) Western blotting with an anti-Flag antibody for detecting LRP4ecd-Flag; and anti-myc antibody for agrin-myc and MuSK-myc. All the transfected cDNAs were similarly expressed. (**E** and **F**) *In vitro* plate-binding assays. Plates were coated with the wild-type or mutant LRP4ecd-Flag protein and overlaid with purified agrin-mycAP protein (E) and MuSKect-mycAP (F). The EK and RH mutants reduce binding affinities for MuSKect-mycAP and agrin-mycAP. Mean and SE are plotted ($n = 4$; $P < 0.05$ for both MuSKect-mycAP and agrin-mycAP by two-way ANOVA).

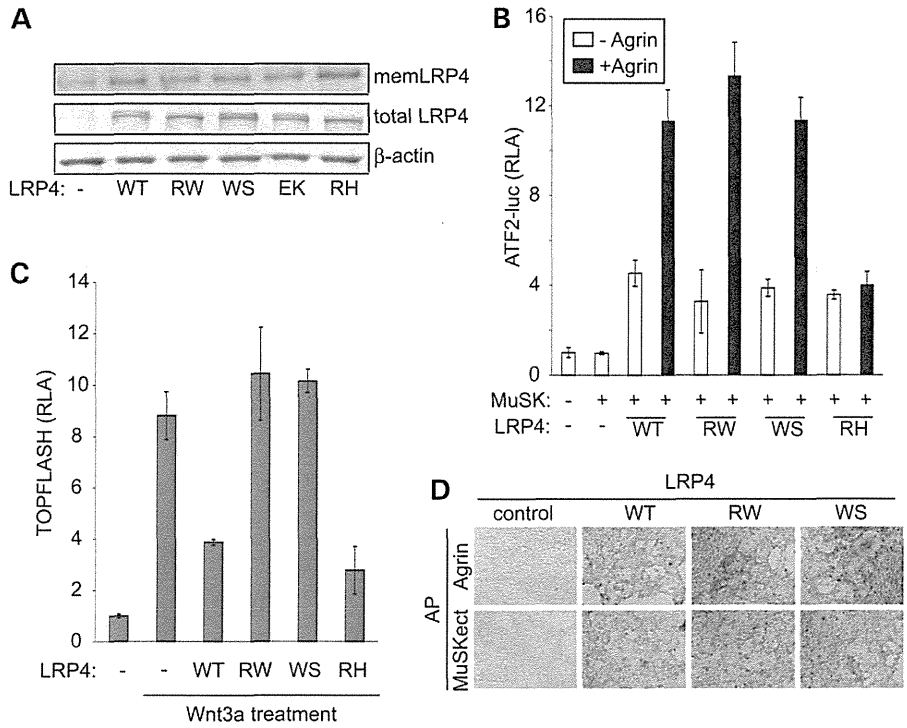

Figure 6. The p.Arg1170Trp (RW) and p.Trp1186Ser (WS) mutants retain the activity of agrin-mediated upregulation of MuSK signaling but compromise Wnt-suppressive activity. (**A**) Western blotting with an anti-Flag antibody for detecting full-length LRP4-Flag. Membrane proteins are biotinylated and precipitated with streptavidin. β-Actin proteins in each sample were detected as loading control. (**B** and **C**) ATF2-luciferase (B) and TPOFLASH (C) reporter assays of HEK293 cells to quantify activation of MuSK and Wnt signaling pathways, respectively. The RH mutant is included as a control. Means and SD of three independent experiments are indicated. (**D**) Cell surface-binding assays as in Figs 5A and B. Both the RW and WS mutants are able to bind to agrin-mycAP (upper) and MuSKect-mycAP (lower).

The diverse array of binding partners enables LRP4 to play an essential role in multiple biological processes including limb and kidney morphogenesis (16,31); bone development through cell fate decision and migration (35); and synaptogenesis (6,34). The multiple phenotypes caused by mutations in the 3rd β-propeller domain prompted us to scrutinize different regions of this domain, and we found that the edge mediates MuSK signaling and the central cavity mediates Wnt signaling. That a single missense mutation in the 3rd β-propeller domain compromises LRP4 binding to MuSK supports a previous observation that MuSK is bound to the 3rd β-propeller domain of LRP4 (Fig. 7B and Supplementary Material, Movie S1) (4). In contrast, reduced binding of our LRP4 mutants to agrin was unexpected because agrin binds to the EGF-like domain, LDLa repeats 6–8 and the 1st β-propeller domain (4,23). The 2nd and 3rd β-propeller domains, however, enhance binding to agrin to ~170% of the truncated LRP4 lacking these domains (4). Accordingly, mutations in the 3rd β-propeller domain in our patient are likely to compromise the enhancing effect conferred by the 3rd β-propeller domain of LRP4.

MATERIALS AND METHODS

Patient

All human studies were in accord with and approved by the Institutional Review Boards of the Mayo Clinic and Nagoya University Graduate School of Medicine. The patient's father gave informed consent for the patient to participate in the study. Venous blood sample was obtained from the patient and his father and genomic DNA was isolated with the QIAamp Blood DNA kit (Qiagen) according to the manufacturer's recommendations.

Neuromuscular junction studies

Intercostal muscle specimens were obtained from the patient and from control subjects without muscle disease undergoing thoracic surgery. Cryosections were used to colocalize the acetylcholine receptor (AChR) and acetylcholine esterase (AChE) as described (36). AChE was also visualized on teased, glutaraldehyde-fixed muscle fibers cytochemically (37). EPs were localized for electron microscopy (38) and quantitatively analyzed (39) by established methods. Peroxidase-labeled α-bgt was used for the ultrastructural localization of AChR (40). The number of AChRs per EP was measured with [^{125}I]α-bgt. The amplitude of the miniature EP potential (MEPP) and EP potential (EPP) amplitudes and estimates of the quantal content of the EPP (*m*) were measured as previously described (41,42). Single-channel patch-clamp recordings were performed as previously described (43,44).

Exome-capture resequencing analysis

We enriched exonic fragments using the SureSelect human all exon v2 (Agilent Technologies) and sequenced 50 bp of each

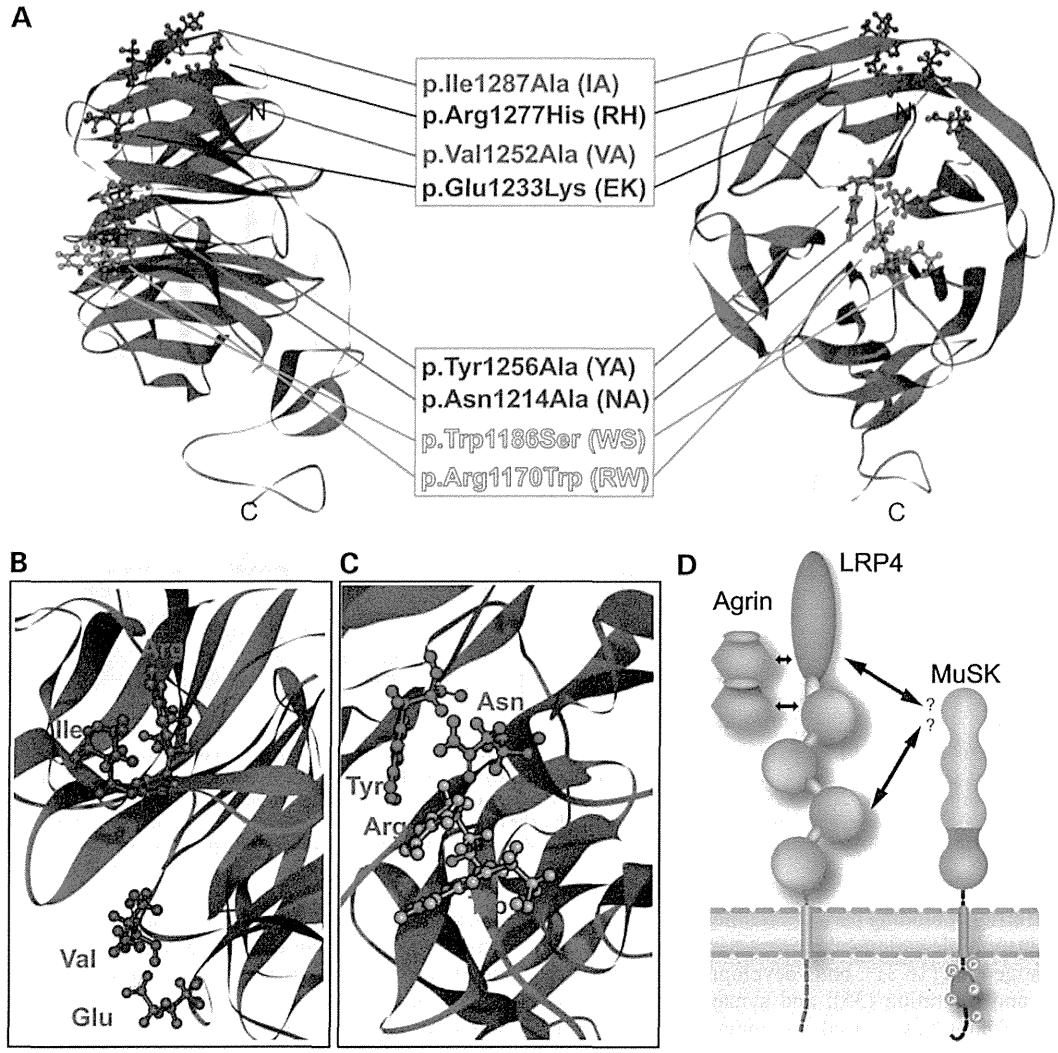

Figure 7. The 3rd β-propeller domain of LRP4 and scheme of agrin/LRP4/MuSK complex. (**A**–**C**) Simulated three-dimensional structure of the 3rd β-propeller domain of LRP4. Positions of the analyzed mutations are indicated. The RH and EK mutations (red) are identified in our CMS patient. The RW and WS mutations (yellow) are reported in sclerosteosis-2 (12). Amino acids that are artificially mutated to alanine are shown in purple or green. Mutations at the edge of the β-propeller domain and in the central cavity are grouped together by boxes. The edge (B) and central cavity (C) of the 3rd β-propeller domain are enlarged to show locations of the naturally occurring and artificially introduced mutations. The viewing positions of (B) and (C) are not identical to (A). (**D**) Scheme of agrin/LRP4/MuSK. Arrows represent direct interactions: Agrin binds to the 1st EGF-like domain and the 1st β-propeller domain of LRP4 (23); MuSK binds to the 4th/5th LDLa repeats and the 3rd β-propeller domain of LRP4 (4). An artificial missense mutation in the 1st IgG-like domain of MuSK impairs binding to LRP4 (4) and deletion of this domain abolishes agrin-mediated AChR clustering (24), but the exact LRP4-binding domain(s) of MuSK remain elusive. We propose that the edge of the 3rd β-propeller domain of LRP4 is essential for binding to MuSK and for signal transduction at NMJ.

fragment in a single direction using ABI SOLiD4 system (Life Technologies). The sequencing fragments were mapped to the human genome hg19/GRCh37 using BioScope 1.4 (Life Technologies). SNVs/indels were called by Avadis NGS 1.3.1 (Agilent) using default parameters. We restricted our analysis to 34 candidate genes that were known to be essential for neuromuscular signal transmission: *ABL2*, *ACHE*, *AGRN*, *APP*, *CHAT*, *CHRNA1*, *CHRNB1*, *CHRND*, *CHRNE*, *CHRNG*, *COLQ*, *CSNK2B*, *DAG1*, *DOK7*, *DTNA*, *DVL1*, *ETV5*, *GFPT1*, *LAMB2*, *LRP4*, *MUSK*, *NRG1*, *NTF4*, *PAK1*, *PGGT1B*, *PHLDB2*, *PLEC*, *RAPSN*, *SCN4A*, *SLC18A3*, *SNTB2*, *STNA1* and *SYNC*.

Primer pairs for each exon and the flanking intron regions of *LRP4* were designed with Primer 3. PCR products were directly sequenced with ABI PRISM 3730 DNA Analyzer and BigDye Terminator Cycle Sequencing Kit version 1.1 according to the manufacturer's protocols (Applied Biosystems).

Plasmids

Full-length human *LRP4* cDNA (Open Biosystems) was cloned into the *Eco*RI site of the pcDNA3.1 mammalian expression vector. The extracellular domain (amino acid 1–1722) of

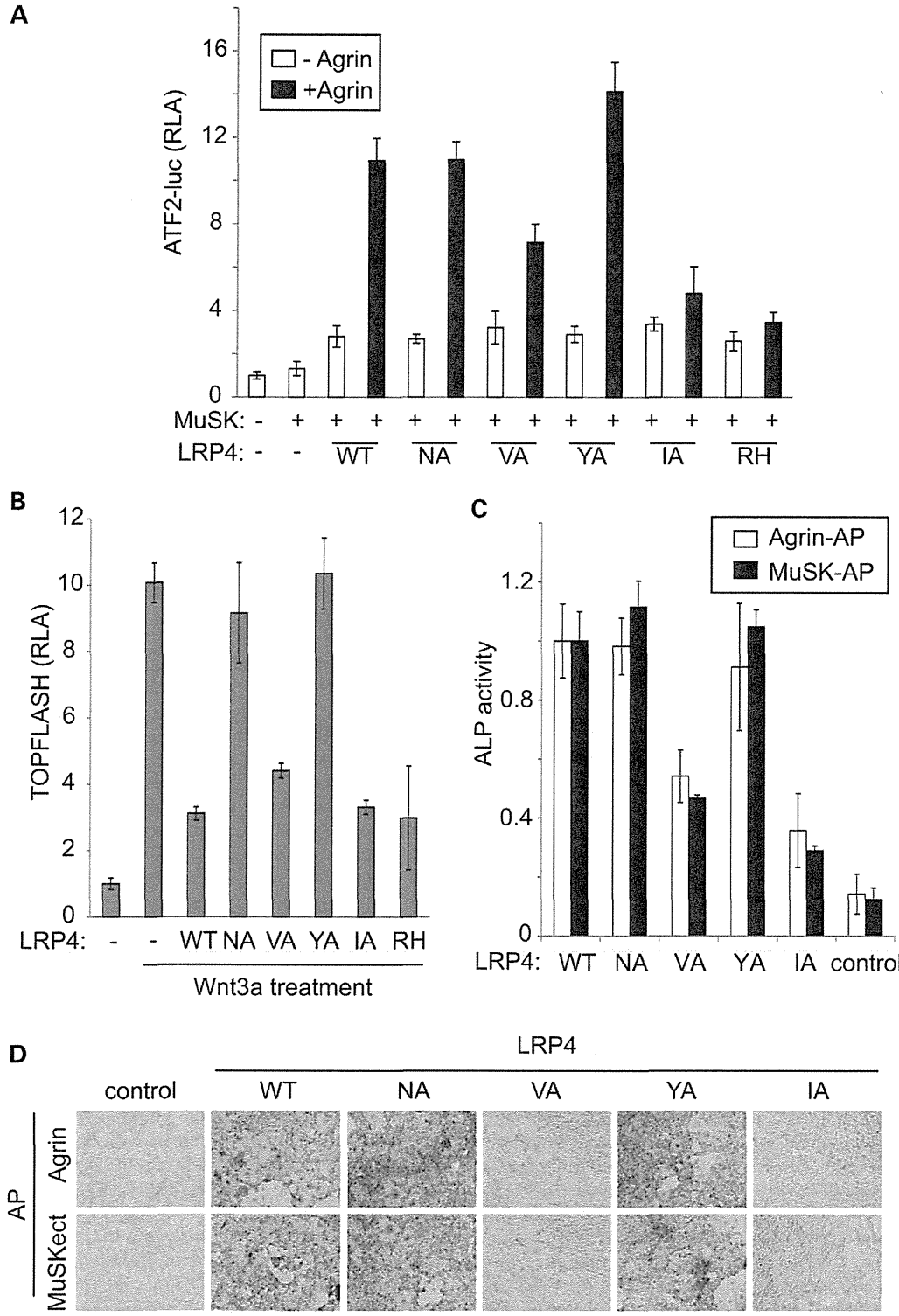

Figure 8. Artificially engineered p.Val1252Ala (VA) and p.Ile1287Ala (IA) compromise agrin-mediated upregulation of MuSK signaling, whereas p.Asn1214Ala (NA) and p.Tyr1256Ala (YA) compromise Wnt-suppressive activity. (**A**) ATF2-luciferase reporter assay of HEK293 cells as in Figs 3A and 6B. The IA and VA mutations are at the edge, whereas the YA and NA mutations are in the central cavity (see Fig. 7A and Supplementary Material, Movie S1). The RH mutation in our CMS patient is included as a control. (**B**) TOPFLASH reporter assay of HEK293 cells as in Figs 3C and 6C. (**C and D**) Cell surface-binding assays as in Figs 5A, B, and 6D. The ALP activities of bound agrin-mycAP and MuSKect-mycAP in three independent wells are shown in (C). Mean and SD are indicated in (A)–(C).

human *LRP4* cDNA was cloned into the *Hin*dIII and *Xba*I sites upstream of a 3xFlag epitope of a mammalian expression vector p3xFlag-CMV-14 to generate hLRP4ecd-Flag for the plate-binding assay. The mouse *Musk* cDNA in pExpress-1 was purchased from Open Biosystems and was used for the luciferase assay in HEK293 cells. Human *MUSK* cDNA with a Flag-tag at the N-terminal end was cloned into the *Eco*RI and *Xba*I sites of the p3xFlag-CMV-14 to generate Flag-MuSK, and was used for the co-immunoprecipitation assay. For vector expressing shRNA against Lrp4, double-stranded oligonucleotides (sense, 5′-GATCCCGGAAGTTTCCTGACATAAATTCAAGAGAT TTATGTCAGGAAACTTCCTTTTGGAAA-3′ and 5′-AGCT TTTCCAAAAAGGAAGTTTCCTGACATAAATCTCTTGAA TTTATGTCAGGAAACTTCCGG-3′) were cloned into a lentiviral vector pLenti-CMV-GFPx2-DEST, which was kindly provided by Dr Eric Campeau at the University of Massachusetts Medical School. The extracellular domain of mouse *Musk* cDNA fused to a myc-tag and alkaline phosphatase (MuSKect-mycAP) was kindly provided by Dr Lin Mei. To generate rat agrin-mycAP that retains potency to facilitate AChR clustering as a neural agrin, we cloned amino acid 1141–1937 of rat *Agrn* cDNA (M64780.1) into pAPtag-5 (GenHunter) at the *Hin*dIII and *Sna*BI sites, so that the Igk-originated signal peptide is attached upstream of the insert and the myc-tag/alkaline phosphatase downstream. Mutant *LRP4* plasmids carrying p.Arg1170Trp, p.Trp1186Ser, p.Asn1214Ala, p.Glu1233Lys, p.Val1252Ala, p.Tyr1256Ala, p.Arg1277His and p.Ile1287Ala were generated by the QuikChange Site-Directed Mutagenesis kit (Stratagene). Lack of PCR artifacts was verified by sequencing the entire inserts. Super 8x TOPFLASH plasmid (Addgene), ATF2-Luc (21) and phRL-TK Renilla luciferase vector (Promega) were used for the luciferase reporter assay.

Cell cultures

HEK293, L, COS and C2C12 cells were cultured in the Dulbecco's modified Eagle's medium (DMEM) supplemented with 10% fetal calf serum and transfected with FuGENE 6 transfection reagent (Roche). L cells stably expressing Wnt3a were purchased from ATCC. Conditioned media were prepared by culturing Wnt3a-producing and control L cells for 4 days. The LRP4ecd-Flag, agrin-mycAP and MuSKect-mycAP proteins were produced by transfecting each plasmid into HEK293 cells in serum-free DMEM. Recombinant rat C-terminal agrin (10 ng/ml, R&D systems) was used for agrin treatment except for the binding assays. For AChR clustering assay, C2C12 myoblast were seeded on a plate coated with collagen I (BD Biosciences) and differentiated in DMEM supplemented with 2% horse serum for 5 days. The differentiated myotubes were electroporated with shLrp4 and each LRP4 cDNA construct using the NEPA21 electroporator and the CUY900-13-3-5 electrode for attached cells (NepaGene), and then treated with 2 μg/ml doxycycline for 2 days to induce shRNA expression. Cells were treated with 10 ng/ml agrin to induce AChR clusters for 12 h. Cells were stained with 10 mg/ml Axexa594-conjugated α-bungarotoxin (1:100, Invitrogen) to label AChR and fixed in 2% paraformaldehyde. Fluorescence images were observed under an Olympus XL71 fluorescence microscope and analyzed with MetaMorph software (Molecular Devices). The lengths of AChR clusters and myotubes were defined as the longest axes of Alexa594 signals and GFP signals, respectively, in the transfected cells. AChR clusters with the axis length <4 μm were excluded from the analysis.

Luciferase assays

HEK293 cells were transfected with ATF2-Luc and phRL-TK along with the *MUSK* and *LRP4* cDNAs. Cells were cultured for 24 h in the presence or absence of agrin in the medium in a 96-well plate. Cells were lysed with the passive lysis buffer (Promega) and assayed for the luciferase activity using the Dual luciferase system (Promega). Each experiment was done in triplicate.

Biotinylation of LRP4 on plasma membrane and western blotting

HEK293 cells transfected with MuSK and LRP4 plasmids in the presence of agrin were cultured for 24 h. C2C12 myoblasts transfected with shLrp4 and human *LRP4* cDNA using NEPA21 electroporator and electroporation cuvettes (NepaGene) were cultured in a differentiation medium for 2 days in the presence of 2 μg/ml doxycycline and 10 ng/ml agrin. Efficient downregulation of Lrp4 was confirmed by quantitative RT–PCR. Cells were lysed with a buffer containing 50 mM HEPES pH 7.0, 150 mM NaCl, 10% glycerol, 1% Triton X-100, 1.5 mM $MgCl_2$, 1 mM EGTA, 100 mM NaF, 10 mM sodium pyrophosphate, 1 μg/μl aprotinin, 1 μg/μl leupeptin, 1 μg/μl pepstatin A, 1 mM PMSF, 1 mM sodium orthovanadate. Cell lysates were subjected to coimmunoprecipitation using 1 μg of anti-phosphotyrosine antibody (4G10, Upstate) attached to protein G Sepharose beads (GE Healthcare). For biotinylation of LRP4 on plasma membrane, LRP4-transfected HEK293 cells were washed twice with PBS containing 1 mM $MgCl_2$ and 0.1 mM $CaCl_2$ (PBS/CM), followed by incubation with 0.5 mg/ml sulfo-NHS-SS-biotin (Pierce) in PBS/CM at room temperature for 30 min. The cells were then washed once with PBS/CM and incubated with 10 mM monoethanolamine for quenching free biotin. The cells were harvested with RIPA buffer (Pierce) after several washing with ice-cold PBS and the cell lysates were incubated with streptavidin sepharose beads (GE healthcare) to purify cell membrane protein. Total or precipitated proteins were dissolved in 1 × laemmli buffer, separated on a 10 or 7.5% SDS–polyacrylamide gel and transferred to a polyvinylidene fluoride membrane (Immobilon-P, Millipore). Membranes were washed in Tris-buffered saline containing 0.05% Tween 20 (TBS-T) and blocked for 1 h at room temperature in TBS-T with 3% bovine serum albumin. The membranes were incubated overnight at 4°C either with the mouse monoclonal anti-Myc 9E10 (dilution 1:500, sc-40, Santa Cruz Biotechnology), anti-Flag M2 (dilution 1:4000, F1804, Sigma-Aldrich), anti-LRP4 (dilution 1:1000, ab85697, Abcam), anti-MuSK (1:500, sc-6009, Santa Cruz Biotechnology) or anti-β-actin (dilution 1:200, sc-47778, Santa Cruz Biotechnology) antibody. The membranes were washed three times for 10 min with TBS-T and incubated with secondary goat anti-mouse IgG antibody conjugated to horseradish peroxidase (HRP) (1:6000, LNA931 V/AG, GE Healthcare) for 1 h at room temperature. The blots were detected with Amersham ECL western blotting detection reagents (GE Healthcare) and quantified with the ImageJ program.

Preparation of agrin-MycAP, MuSKect-MycAP and LRP4ecd-flag proteins

Agrin-mycAP and MuSKect-mycAP in the conditioned media of transfected HEK293 cells were concentrated ~100-fold using Amicon Ultra-4 filters (Millipore). For the cell surface-binding assay, we used the concentrated conditioned media. For the plate-binding assay, we further purified agrin-mycAP and MuSKect-mycAP using the c-myc-Tagged Protein Mild Purification Kit ver. 2 (MBL). Wild-type and mutant hLRP4ecd-Flag proteins were purified with the Anti-DYKDDDDK-tag Antibody Beads (Wako) from the conditioned medium of the transfected HEK293. Purified MuSKect-mycAP and hLRP4ecd-Flag were detected by anti-myc antibody (9E10, Abcam) or anti-Flag antibody (M2, Sigma-Aldrich), respectively. We also measured concentrations of each protein by SDS–PAGE followed by protein staining with SYBRO Ruby Protein Gel Stain (Molecular Probes) using BSA as a standard.

Cell surface- and plate-binding assays

For the cell surface-binding assay, COS cells were transfected with LRP4 using FuGENE 6 (Roche). Cells were incubated 24 h with concentrated conditioned medium containing either agrin-mycAP or MuSKect-mycAP for 1.5 h at RT. Cells were washed with HABH buffer (0.5 mg/ml bovine serum albumin, 0.1% NaN_3 and 20 mM HEPES, pH 7.0, in Hank's balanced salt solution), fixed in 60% acetone for 10 min on ice followed by 4% paraformaldehyde in 20 mM HEPES (pH 7.0) in Hank's balanced salt solution for 10 min on ice. Fixed cells were washed once with 20 mM HEPES (pH 7.0) and 150 mM NaCl, incubated at 65°C for 30 min, washed with 0.1 M Tris–HCl (pH 8.0), washed with water and stained with NBP/BCIP solution (Roche). For plate-biding assay, the Immuno plate (Nunc) was coated with 0.15 μg of purified wild-type or mutant LRP4ecd-Flag at 4°C overnight and then incubated with a blocking buffer (1%BSA in PBS) at RT for 1 h. For the binding assays, 80 μl of serially diluted agrin-mycAP or MuSKect-mycAP were added to wells that were coated with wild-type or mutant LRP4ecd-Flag in a blocking buffer. The reagents were incubated for 2 h at RT, and then washed twice with PBS. Bound AP activity was measured using LabAssay ALP (Wako).

Homology modeling

The primary sequence of the 3rd β-propeller domain of hLRP4 (accession number: AAI36669, amino acid 1048–1350) and the coordinates of crystal structure of the 1st β-propeller domain (amino acid 20–326) of human LRP6 (PDB ID: 3SOV) were loaded into the Molecular Operating Environment software (MOE, Chemical Computing Group). The primary structures of each β-propeller domain of hLRP4 and hLRP6 were sequence-aligned and manually corrected by the structure–alignment method. Molecular mechanics were calculated by an MMFF94x force field.

SUPPLEMENTARY MATERIAL

Supplementary Material is available at *HMG* online.

ACKNOWLEDGEMENTS

We thank Keiko Itano for expert technical assistance.

Conflict of Interest statement. None declared.

FUNDING

This work was supported by Grants-in-Aid from the MEXT and MHLW of Japan to B.O., M.I., A.M. and K.O.; and by NIH Research Grant NS6277 from the NINDS and by Research Grant from the MDA to A.G.E.

REFERENCES

1. Engel, A.G. (2012) Current status of the congenital myasthenic syndromes. *Neuromuscul. Disord.*, **22**, 99–111.
2. Kim, N., Stiegler, A.L., Cameron, T.O., Hallock, P.T., Gomez, A.M., Huang, J.H., Hubbard, S.R., Dustin, M.L. and Burden, S.J. (2008) Lrp4 is a receptor for agrin and forms a complex with MuSK. *Cell*, **135**, 334–342.
3. Zhang, B., Luo, S., Wang, Q., Suzuki, T., Xiong, W.C. and Mei, L. (2008) LRP4 serves as a coreceptor of agrin. *Neuron*, **60**, 285–297.
4. Zhang, W., Coldefy, A.S., Hubbard, S.R. and Burden, S.J. (2011) Agrin binds to the N-terminal region of Lrp4 protein and stimulates association between Lrp4 and the first immunoglobulin-like domain in muscle-specific kinase (MuSK). *J. Biol. Chem.*, **286**, 40624–40630.
5. Wu, H., Xiong, W.C. and Mei, L. (2010) To build a synapse: signaling pathways in neuromuscular junction assembly. *Development*, **137**, 1017–1033.
6. Yumoto, N., Kim, N. and Burden, S.J. (2012) Lrp4 is a retrograde signal for presynaptic differentiation at neuromuscular synapses. *Nature*, **489**, 438–442.
7. Wu, H., Lu, Y., Shen, C., Patel, N., Gan, L., Xiong, W.C. and Mei, L. (2012) Distinct roles of muscle and motoneuron LRP4 in neuromuscular junction formation. *Neuron*, **75**, 94–107.
8. Higuchi, O., Hamuro, J., Motomura, M. and Yamanashi, Y. (2011) Autoantibodies to low-density lipoprotein receptor-related protein 4 in myasthenia gravis. *Ann. Neurol.*, **69**, 418–422.
9. Zhang, B., Tzartos, J.S., Belimezi, M., Ragheb, S., Bealmear, B., Lewis, R.A., Xiong, W.C., Lisak, R.P., Tzartos, S.J. and Mei, L. (2012) Autoantibodies to lipoprotein-related protein 4 in patients with double-seronegative myasthenia gravis. *Arch. Neurol.*, **69**, 445–451.
10. Pevzner, A., Schoser, B., Peters, K., Cosma, N.C., Karakatsani, A., Schalke, B., Melms, A. and Kroger, S. (2012) Anti-LRP4 autoantibodies in AChR- and MuSK-antibody-negative myasthenia gravis. *J. Neurol.*, **259**, 427–435.
11. Li, Y., Pawlik, B., Elcioglu, N., Aglan, M., Kayserili, H., Yigit, G., Percin, F., Goodman, F., Nurnberg, G., Cenani, A. *et al.* (2010) LRP4 mutations alter Wnt/beta-catenin signaling and cause limb and kidney malformations in Cenani–Lenz syndrome. *Am. J. Hum. Genet.*, **86**, 696–706.
12. Leupin, O., Piters, E., Halleux, C., Hu, S., Kramer, I., Morvan, F., Bouwmeester, T., Schirle, M., Bueno-Lozano, M., Fuentes, F.J. *et al.* (2011) Bone overgrowth-associated mutations in the LRP4 gene impair sclerostin facilitator function. *J. Biol. Chem.*, **286**, 19489–19500.
13. Styrkarsdottir, U., Halldorsson, B.V., Gretarsdottir, S., Gudbjartsson, D.F., Walters, G.B., Ingvarsson, T., Jonsdottir, T., Saemundsdottir, J., Snorradottir, S., Center, J.R. *et al.* (2009) New sequence variants associated with bone mineral density. *Nat. Genet.*, **41**, 15–17.
14. Choi, H.Y., Dieckmann, M., Herz, J. and Niemeier, A. (2009) Lrp4, a novel receptor for Dickkopf 1 and sclerostin, is expressed by osteoblasts and regulates bone growth and turnover in vivo. *PLoS ONE*, **4**, e7930.
15. Johnson, E.B., Steffen, D.J., Lynch, K.W. and Herz, J. (2006) Defective splicing of Megf7/Lrp4, a regulator of distal limb development, in autosomal recessive mulefoot disease. *Genomics*, **88**, 600–609.
16. Johnson, E.B., Hammer, R.E. and Herz, J. (2005) Abnormal development of the apical ectodermal ridge and polysyndactyly in Megf7-deficient mice. *Hum. Mol. Genet.*, **14**, 3523–3538.
17. Rasi, S., Spina, V., Bruscaggin, A., Vaisitti, T., Tripodo, C., Forconi, F., De Paoli, L., Fangazio, M., Sozzi, E., Cencini, E. *et al.* (2011) A variant of the LRP4 gene affects the risk of chronic lymphocytic leukaemia transformation to Richter syndrome. *Br. J. Haematol.*, **152**, 284–294.

18. Adzhubei, I.A., Schmidt, S., Peshkin, L., Ramensky, V.E., Gerasimova, A., Bork, P., Kondrashov, A.S. and Sunyaev, S.R. (2010) A method and server for predicting damaging missense mutations. *Nat. Methods*, **7**, 248–249.
19. Kumar, P., Henikoff, S. and Ng, P.C. (2009) Predicting the effects of coding non-synonymous variants on protein function using the SIFT algorithm. *Nat. Protoc.*, **4**, 1073–1081.
20. Schwarz, J.M., Rodelsperger, C., Schuelke, M. and Seelow, D. (2010) MutationTaster evaluates disease-causing potential of sequence alterations. *Nat. Methods*, **7**, 575–576.
21. Ohkawara, B. and Niehrs, C. (2011) An ATF2-based luciferase reporter to monitor non-canonical Wnt signaling in Xenopus embryos. *Dev. Dyn.*, **240**, 188–194.
22. Okada, K., Inoue, A., Okada, M., Murata, Y., Kakuta, S., Jigami, T., Kubo, S., Shiraishi, H., Eguchi, K., Motomura, M. *et al.* (2006) The muscle protein Dok-7 is essential for neuromuscular synaptogenesis. *Science*, **312**, 1802–1805.
23. Zong, Y., Zhang, B., Gu, S., Lee, K., Zhou, J., Yao, G., Figueiredo, D., Perry, K., Mei, L. and Jin, R. (2012) Structural basis of agrin-LRP4-MuSK signaling. *Genes. Dev.*, **26**, 247–258.
24. Zhou, H., Glass, D.J., Yancopoulos, G.D. and Sanes, J.R. (1999) Distinct domains of MuSK mediate its abilities to induce and to associate with postsynaptic specializations. *J. Cell Biol.*, **146**, 1133–1146.
25. Huze, C., Bauche, S., Richard, P., Chevessier, F., Goillot, E., Gaudon, K., Ben Ammar, A., Chaboud, A., Grosjean, I., Lecuyer, H.A. *et al.* (2009) Identification of an agrin mutation that causes congenital myasthenia and affects synapse function. *Am. J. Hum. Genet.*, **85**, 155–167.
26. Chevessier, F., Faraut, B., Ravel-Chapuis, A., Richard, P., Gaudon, K., Bauche, S., Prioleau, C., Herbst, R., Goillot, E., Ioos, C. *et al.* (2004) MUSK, a new target for mutations causing congenital myasthenic syndrome. *Hum. Mol. Genet.*, **13**, 3229–3240.
27. Selcen, D., Fukuda, T., Shen, X.-M. and Engel, A.G. (2004) Are MuSK antibodies the primary cause of myasthenic symptoms? *Neurology*, **62**, 1945–1950.
28. Shiraishi, H., Motomura, M., Yoshimura, T., Fukudome, T., Fukuda, T., Nakao, Y., Tsujihata, M., Vincent, A. and Eguchi, K. (2005) Acetylcholine receptors loss and postsynaptic damage in MuSK antibody-positive myasthenia gravis. *Ann. Neurol.*, **57**, 289–293.
29. Punga, A.R., Maj, M., Lin, S., Meinen, S. and Ruegg, M.A. (2011) MuSK levels differ between adult skeletal muscles and influence postsynaptic plasticity. *Eur. J. Neurosci.*, **33**, 890–898.
30. Bao, J., Zheng, J.J. and Wu, D. (2012) The structural basis of DKK-mediated inhibition of Wnt/LRP signaling. *Sci. Signal*, **5**, pe22.
31. Karner, C.M., Dietrich, M.F., Johnson, E.B., Kappesser, N., Tennert, C., Percin, F., Wollnik, B., Carroll, T.J. and Herz, J. (2010) Lrp4 regulates initiation of ureteric budding and is crucial for kidney formation–a mouse model for Cenani-Lenz syndrome. *PLoS ONE*, **5**, e10418.
32. Glinka, A., Wu, W., Delius, H., Monaghan, A.P., Blumenstock, C. and Niehrs, C. (1998) Dickkopf-1 is a member of a new family of secreted proteins and functions in head induction. *Nature*, **391**, 357–362.
33. Semenov, M., Tamai, K. and He, X. (2005) SOST is a ligand for LRP5/LRP6 and a Wnt signaling inhibitor. *J. Biol. Chem.*, **280**, 26770–26775.
34. Lu, Y., Tian, Q.B., Endo, S. and Suzuki, T. (2007) A role for LRP4 in neuronal cell viability is related to apoE-binding. *Brain Res.*, **1177**, 19–28.
35. Ohazama, A., Johnson, E.B., Ota, M.S., Choi, H.Y., Porntaveetus, T., Oommen, S., Itoh, N., Eto, K., Gritli-Linde, A., Herz, J. *et al.* (2008) Lrp4 modulates extracellular integration of cell signaling pathways in development. *PLoS ONE*, **3**, e4092.
36. Fambrough, D.M., Engel, A.G. and Rosenberry, T.L. (1982) Acetylcholinesterase of human erythrocytes and neuromuscular junctions: homologies revealed by monoclonal antibodies. *Proc. Natl. Acad. Sci. USA*, **79**, 1078–1082.
37. Gautron, J. (1974) Cytochimie ultrastructurale des acétylcholinestérases. *Microscopie*, **21**, 259–264.
38. Engel, A.G. (2004) In Engel, A.G. and Franzini-Armstrong, C. (eds.), *Myology*. 3rd edn. McGraw Hill, New York, Vol. I, pp. 681–690.
39. Engel, A.G. (1994) In Engel, A.G. and Franzini-Armstrong, C. (eds.), *Myology*. 2nd edn. McGraw-Hill, New York, Vol. 2, pp. 1018–1045.
40. Engel, A.G., Lindstrom, J.M., Lambert, E.H. and Lennon, V.A. (1977) Ultrastructural localization of the acetylcholine receptor in myasthenia gravis and in its experimental autoimmune model. *Neurology*, **27**, 307–315.
41. Engel, A.G., Nagel, A., Walls, T.J., Harper, C.M. and Waisburg, H.A. (1993) Congenital myasthenic syndromes: I. Deficiency and short open-time of the acetylcholine receptor. *Muscle Nerve*, **16**, 1284–1292.
42. Uchitel, O., Engel, A.G., Walls, T.J., Nagel, A., Atassi, M.Z. and Bril, V. (1993) Congenital myasthenic syndromes: II. Syndrome attributed to abnormal interaction of acetylcholine with its receptor. *Muscle Nerve*, **16**, 1293–1301.
43. Milone, M., Hutchinson, D.O. and Engel, A.G. (1994) Patch-clamp analysis of the properties of acetylcholine receptor channels at the normal human endplate. *Muscle Nerve*, **17**, 1364–1369.
44. Shen, X.M., Brengman, J.M., Sine, S.M. and Engel, A.G. (2012) Myasthenic syndrome AChRalpha C-loop mutant disrupts initiation of channel gating. *J. Clin. Invest.*, **122**, 2613–2621.

J Mol Neurosci (2014) 53:359–361
DOI 10.1007/s12031-013-0170-x

Collagen Q is a Key Player for Developing Rational Therapy for Congenital Myasthenia and for Dissecting the Mechanisms of Anti-MuSK Myasthenia Gravis

Kinji Ohno · Mikako Ito · Yu Kawakami · Kenji Ohtsuka

Received: 10 October 2013 / Accepted: 31 October 2013 / Published online: 15 November 2013

Abstract Acetylcholinesterase (AChE) at the neuromuscular junction (NMJ) is anchored to the synaptic basal lamina via a triple helical collagen Q (ColQ) in the form of asymmetric AChE (AChE/ColQ). We exploited the proprietary NMJ-targeting signals of ColQ to treat congenital myasthenia and to explore the mechanisms of autoimmune myasthenia gravis (MG). Mutations in *COLQ* cause congenital endplate AChE deficiency (CEAD). First, a single intravenous administration of adeno-associated virus serotype 8 (AAV8)-*COLQ* to *Colq*−/− mice normalized motor functions, synaptic transmission, and partly the NMJ ultrastructure. Additionally, injection of purified recombinant AChE/ColQ protein complex into gluteus maximus accumulated AChE in non-injected forelimbs. Second, MuSK antibody-positive MG accounts for 5–15 % of MG. In vitro overlay of AChE/ColQ to muscle sections of *Colq*−/− mice, as well as in vitro plate-binding of MuSK to ColQ, revealed that MuSK-IgG blocks binding of ColQ to MuSK in a dose-dependent manner. Passive transfer of MuSK-IgG to wild-type mice markedly reduced the size and intensity of ColQ signals at NMJs. MuSK-IgG thus interferes with binding of ColQ to MuSK. Elucidation of molecular mechanisms of specific binding of ColQ to NMJ enabled us to ameliorate devastating myasthenic symptoms of *Colq*−/− mice and also to reveal underlying mechanisms of anti-MuSK-MG.

Keywords Acetylcholinesterase · Collagen Q · MuSK · Congenital myasthenic syndrome · Myasthenia gravis

K. Ohno (✉) · M. Ito · Y. Kawakami · K. Ohtsuka
Division of Neurogenetics, Center for Neurological Diseases and Cancer, Nagoya University Graduate School of Medicine, Nagoya, Japan
e-mail: ohnok@med.nagoya-u.ac.jp

Introduction

Acetylcholinesterase (AChE) at the neuromuscular junction (NMJ) is anchored to the synaptic basal lamina by binding to a triple helical collagen Q (ColQ) in the form of asymmetric AChE (AChE/ColQ) (Fig. 1). AChE/ColQ is localized to the synaptic basal lamina by using two mechanisms. First, the C-terminal domain of ColQ binds to MuSK (Cartaud et al. 2004). Dimeric MuSK binds to dimeric LRP4 at the NMJ, and binding of nerve terminal-derived agrin to LRP4 induces MuSK phosphorylation, which leads to clustering of acetylcholine receptor (AChR) (Kim et al. 2008; Zhang et al. 2008). Although the lack of ColQ decreases membrane-bound MuSK and attenuates agrin-mediated AChR clusters (Sigoillot et al. 2010), the exact role of ColQ on MuSK signaling still remains to be clarified. Second, two heparin-binding domains of ColQ bind to synaptic heparan sulfate proteoglycans including perlecan (Deprez et al. 2003; Kimbell et al. 2004). We here show that the specific anchoring of ColQ to the synaptic basal lamina is exploited to cure congenital endplate AChE deficiency (Ito et al. 2012) and also to explore the molecular mechanisms of anti-MuSK myasthenia gravis (MG) (Kawakami et al. 2011).

Congenital Endplate AChE Deficiency

Mutations in a gene encoding ColQ cause congenital endplate AChE deficiency (CEAD) and a myasthenic syndrome (Ohno et al. 1998). Acetylcholine (ACh) released from the nerve terminal stays at NMJ for an abnormally longer period of time because of the lack of the ACh-hydrolyzing AChE. The prolonged dwell time of ACh at the NMJ causes (a) desensitization of muscle nicotinic acetylcholine receptor (AChR), (b) endplate myopathy due to excessive influx of Ca^{2+} ions into muscle; and (c) depolarization of resting membrane

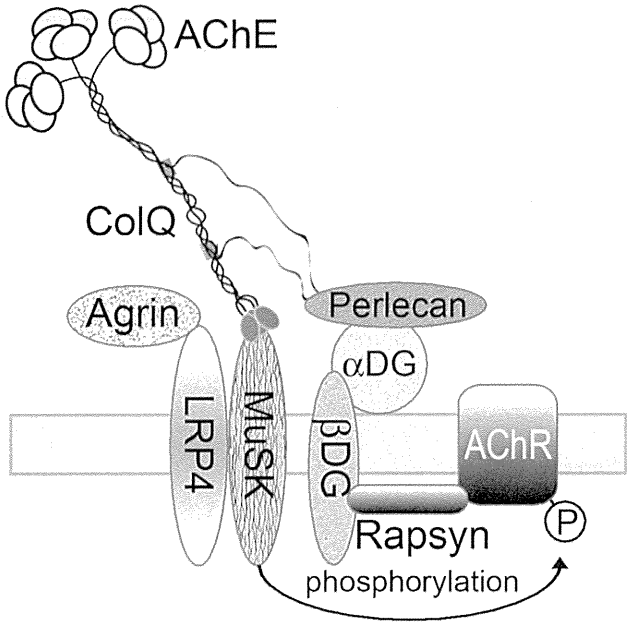

Fig. 1 Scheme of the anchoring of ColQ to NMJ. Twelve catalytic subunits of AChE are attached to triple helical ColQ to form a large AChE/ColQ complex. Two heparin-binding domains in the shaft of ColQ are bound to perlecan. C-terminal domain of ColQ is bound to MuSK. Nerve-derived agrin binds to an LRP4-MuSK complex and induces clustering of AChR by phosphorylating AChR β subunit. Phosphorylated AChRs forms an AChR cluster with a subsynaptic structural protein, rapsyn. *DG*, dystroglycan

potential at the endplate (EP), which is caused by staircase summation of EP potentials. Clinical features include abnormal fatigue due to defective neuromuscular signal transmission. Unlike myasthenia gravis and congenital AChR deficiency, for which cholinesterase inhibitors and 3,4-diaminopyridine are effective, there is no rational therapy for CEAD except for mild to moderate effects of ephedrine (Mihaylova et al. 2008).

Protein-Anchoring Therapy for CEAD

In an effort to explore a therapeutic option for CEAD, we exploited the unique feature of ColQ that specifically anchors to the synaptic basal lamina (Ito et al. 2012). We previously reported that incubation of AChE/ColQ on a section of frog muscle enables specific anchoring of AChE/ColQ to the NMJ (Kimbell et al. 2004). We first confirmed that recombinant human AChE/ColQ was able to bind to mouse NMJs. We next generated an adeno-associated vector serotype 8 (AAV8)-*COLQ* and intravenously administered AAV8-*COLQ* to *Colq*−/− mice at 4 weeks of age. The AAV treatment anchored AChE/ColQ at the NMJ (Fig. 2) and markedly ameliorated motor deficits, abnormal neuromuscular signal transmission, and the degenerative NMJ ultrastructure in 4 weeks. We also observed that the treatment increased the amount of AChE/ColQ in skeletal muscle from 0 to 89 % of wild type, and the ratio of asymmetric AChE/ColQ species became indistinguishable from that of wild type. To confirm that AChE/ColQ indeed moved in the mouse body, we injected AAV1-*COLQ*-IRES-EGFP to the left tibialis anterior of *Colq*−/− mice and observed colocalization of ColQ and AChE at all the examined NMJs in non-injected limbs. Unlike AAV8, AAV1 tends to stay at the injected site and does not go into blood stream. We also confirmed by real-time PCR that the copy numbers of AAV1-*COLQ*-IRES-EGFP in non-injected limbs were 1,300 to 1,700 times less that in the injected limb. Nevertheless, biochemical assays showed that the amount of AChE/ColQ in non-injected limbs became 22 to 28 % of wild type, which indicated that the large AChE/ColQ complex with a predicted molecular weight of ~960 kDa indeed moved from one limb to another. We further tested the travel of AChE/ColQ to remote NMJs by injecting purified recombinant AChE/ColQ protein complex into the gluteus maximus of *Colq*−/− mice for seven continuous days. Histological analysis revealed that AChE/ColQ was present at all the examined NMJs of triceps muscles. Furthermore, the ColQ signal intensity normalized for the AChR area reached 42 % of wild type. The protein-injected mice also acquired the ability to hang on the wire for two or more minutes. We also observed that intravenous injection of AAV8-*COLQ* infected a large number of liver cells, but cytochemical and immunological staining did not detect AChE/ColQ in the liver. Similarly, we did not detect AChE/ColQ in the kidney glomerular basement membrane. Lack of ectopic anchoring of AChE/ColQ also

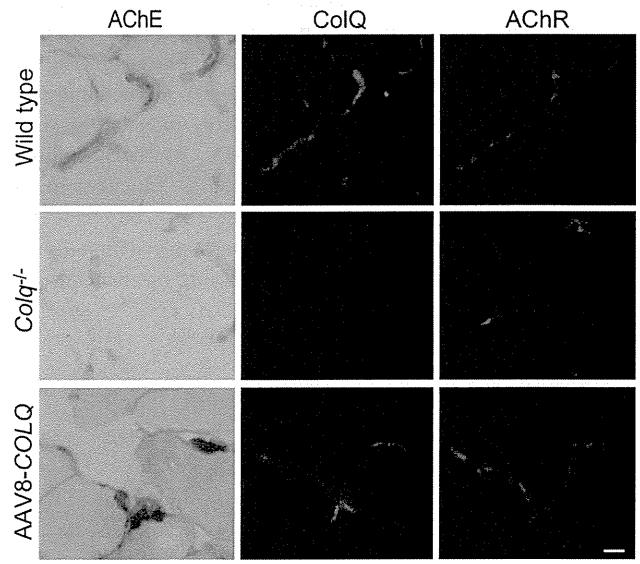

Fig. 2 Histology of NMJs treated with AAV8-*COLQ*. Localization of AChE, ColQ, and AChR in quadriceps muscles of wild type, untreated *Colq*−/−, and AAV8-*COLQ*-treated *Colq*−/− mice. Mice are intravenously injected with 2×10^{12} vg of AAV8-*COLQ*. AChE is stained for its activity and the nuclei are simultaneously stained with hematoxylin. ColQ and AChR are detected by anti-ColQ antibody and α-bungarotoxin, respectively. *Bar* = 10 μm

underscored a notion that AChE/ColQ was specifically targeted to the NMJ where the binding partners of perlecan and MuSK were expressed. Application of gene therapy in clinical practice is usually hampered by the lack of a modality to precisely deliver the transgene to a target organ. As has been observed in ColQ, extracellular matrix proteins are expected to have proprietary protein-anchoring domains, which enable specific tissue targeting. The protein-anchoring therapy thus can be potentially applied to a wide range of congenital and acquired defects of extracellular matrix proteins.

Anti-MuSK Myasthenia Gravis

MG is caused by autoantibodies against molecules expressed at the NMJ. About 80 % of MG is caused by anti-AChR antibody, whereas 5 to 15 % are caused by anti-MuSK antibody (Farrugia et al. 2006; Farrugia and Vincent 2010). Autoantibody against LRP4 also accounts for MG, but its pathogenicity has not been proven by passive transfer of patient's antibody or active immunization using model animals (Higuchi et al. 2011). MuSK-MG patients respond favorably to immunotherapy, but usually do not respond to or are even worsened by cholinesterase inhibitors (Pasnoor et al. 2010). Anti-AChR antibodies comprise IgG1 and IgG3 that recruit complements, whereas anti-MuSK antibodies largely comprise IgG4 that do not activate complements (McConville et al. 2004). The exact target blocked by anti-MuSK-IgG, however, remained unsolved.

MuSK-IgG Blocks Anchoring of ColQ to MuSK

Being prompted by lack of the effect of cholinesterase inhibitors in MuSK-MG patients and also by the fact that MuSK-IgG is a blocking antibody, we hypothesized that MuSK-IgG blocks binding of ColQ and MuSK. We first confirmed that human MuSK-IgG recognizes the normal mouse NMJ. In vitro overlay of purified recombinant AChE/ColQ to muscle sections of *Colq*−/− mice revealed that MuSK-IgG blocks binding of ColQ to MuSK (Kawakami et al. 2011). In vitro plate-binding of purified recombinant MuSK to purified recombinant AChE/ColQ demonstrated that MuSK-IgG blocks binding of MuSK and AChE/ColQ in a dose-dependent manner. In addition, passive transfer of MuSK-IgG to C57BL/6J mice reduced the size and density of ColQ signals to ~10 % of controls and those of AChR and MuSK signals to 30–50 % of controls. We also found that MuSK-IgG does not block binding of MuSK and LRP4 in the absence of agrin. In the presence of agrin, however, MuSK-IgG blocked binding of MuSK and LRP4. Thus, MuSK-IgG is likely to compromise the NMJ signal transmission by blocking the anchoring of the AChE/ColQ complex and by impairing the agrin/LRP4/MuSK signaling pathway.

Conclusions

Elucidation of molecular mechanisms of specific binding of ColQ to the NMJ enabled us to ameliorate the devastating myasthenic symptoms of *Colq*−/− mice and also to reveal underlying mechanisms of anti-MuSK MG.

Acknowledgments The current studies were supported by grants-in-aid from MEXT and NHLW of Japan.

References

Cartaud A, Strochlic L, Guerra M et al (2004) MuSK is required for anchoring acetylcholinesterase at the neuromuscular junction. J Cell Biol 165:505–515

Deprez P, Inestrosa NC, Krejci E (2003) Two different heparin-binding domains in the triple-helical domain of ColQ, the collagen tail subunit of synaptic acetylcholinesterase. J Biol Chem 278:23233–23242

Farrugia ME, Vincent A (2010) Autoimmune mediated neuromuscular junction defects. Curr Opin Neurol 23:489–495

Farrugia ME, Robson MD, Clover L et al (2006) MRI and clinical studies of facial and bulbar muscle involvement in MuSK antibody-associated myasthenia gravis. Brain 129: 1481–1492

Higuchi O, Hamuro J, Motomura M, Yamanashi Y (2011) Autoantibodies to low-density lipoprotein receptor-related protein 4 in myasthenia gravis. Ann Neurol 69:418–422

Ito M, Suzuki Y, Okada T et al (2012) Protein-anchoring strategy for delivering acetylcholinesterase to the neuromuscular junction. Mol Ther 20:1384–1392

Kawakami Y, Ito M, Hirayama M et al (2011) Anti-MuSK autoantibodies block binding of collagen Q to MuSK. Neurology 77:1819–1826

Kim N, Stiegler AL, Cameron TO et al (2008) Lrp4 is a receptor for agrin and forms a complex with MuSK. Cell 135:334–342

Kimbell LM, Ohno K, Engel AG, Rotundo RL (2004) C-terminal and heparin-binding domains of collagenic tail subunit are both essential for anchoring acetylcholinesterase at the synapse. J Biol Chem 279: 10997–11005

McConville J, Farrugia ME, Beeson D et al (2004) Detection and characterization of MuSK antibodies in seronegative myasthenia gravis. Ann Neurol 55:580–584

Mihaylova V, Muller JS, Vilchez JJ et al (2008) Clinical and molecular genetic findings in COLQ-mutant congenital myasthenic syndromes. Brain 131:747–759

Ohno K, Brengman J, Tsujino A, Engel AG (1998) Human endplate acetylcholinesterase deficiency caused by mutations in the collagen-like tail subunit (ColQ) of the asymmetric enzyme. Proc Natl Acad Sci U S A 95:9654–9659

Pasnoor M, Wolfe GI, Nations S et al (2010) Clinical findings in MuSK-antibody positive myasthenia gravis: a U.S. experience. Muscle Nerve 41:370–374

Sigoillot SM, Bourgeois F, Lambergeon M, Strochlic L, Legay C (2010) ColQ controls postsynaptic differentiation at the neuromuscular junction. J Neurosci 30:13–23

Zhang B, Luo S, Wang Q, Suzuki T, Xiong WC, Mei L (2008) LRP4 serves as a coreceptor of agrin. Neuron 60:285–297

CHAPTER

37

Lysosomal Membrane Disorders: LAMP-2 Deficiency

Kazuma Sugie[*,†] *and Ichizo Nishino*[†]

[*]Nara Medical University School of Medicine, Nara, Japan
[†]National Center of Neurology and Psychiatry, Tokyo, Japan

INTRODUCTION

In normal skeletal muscle, lysosomes have morphologically unremarkable structures. By electron microscopy they are very hard to find and appear to be totally devoid of internal structures compared to other organelles such as mitochondria. Nevertheless, lysosomes have important physiological roles in skeletal muscle, since a number of muscle diseases are accompanied by structurally abnormal lysosomes. Among these disorders, two have been genetically defined, acid maltase deficiency and Danon disease. This chapter will focus on the latter disease, which is due to a primary deficiency of lysosome-associated membrane protein-2 (LAMP-2). To date, this is the only known human muscle disorder caused by a lysosomal membrane protein defect.

DANON DISEASE

In 1981, Danon and colleagues reported two unrelated 16-year-old boys with similar phenotypes[1] characterized by the clinical triad of hypertrophic cardiomyopathy, myopathy, and mental retardation. In addition to these clinical manifestations, the disorder was characterized by a vacuolar myopathy with increased muscle glycogen, resembling glycogen-storage disease type II; however, acid maltase activity was normal. Accordingly, the disease was called "lysosomal glycogen-storage disease with normal acid maltase." However, the disease is not a glycogen-storage disease because glycogen is not always increased and because the defective molecule, LAMP-2, is a structural protein rather than a glycogenolytic enzyme.[2] Therefore, "Danon disease" has been redefined as X-linked vacuolar cardiomyopathy and myopathy due to LAMP-2 deficiency.[2]

CLINICAL FEATURES

Clinically, the disease is characterized by hypertrophic cardiomyopathy, myopathy, and mental retardation.[2,3] All probands were male, but females had milder and later-onset cardiomyopathy; therefore, the disease was thought to be transmitted as an X-linked dominant mode trait, even before the underlying defect was identified. In fact, the causative gene for Danon disease, *LAMP-2*, is on chromosome Xq24.[4]

Pregnancies and deliveries are usually normal. Ages at onset in a study of 20 male and 18 female patients varied from 10 months to 19 years in males and from 12 to 53 years in females.[3] The actual onset can be earlier, but symptoms may remain undetected because of the subacute, insidious nature and slow progression of the disease. For example, two male patients were identified only when isolated increases in serum creatine kinase (CK) were noted, and two

Rosenberg's Molecular and Genetic Basis of Neurological and Psychiatric Disease
http://dx.doi.org/10.1016/10.1016/B978-0-12-410529-4.00037-1

other patients were considered to have Danon disease because they had abnormal electrocardiograms (ECGs) before they showed any cardiac symptoms. Most commonly, onset is in childhood, but one male patient developed dyspnea in the infantile period. Delayed milestones with mild mental retardation have been observed in 15% of male patients.

Sooner or later, all patients develop cardiomyopathy, which is the most severe and life-threatening manifestation. In male patients, cardiac symptoms, such as exertional dyspnea, begin during the teenage years. Hypertrophic cardiomyopathy predominates in males, while dilated cardiomyopathy is more common in females. However, male patients can also show dilated cardiomyopathy, especially later in their lives. Cardiac arrhythmia, especially Wolff–Parkinson–White (WPW) syndrome, is often seen in both males and females. In a study of 38 patients with genetically confirmed Danon disease, ages at death were 19±6 (mean±standard deviation [SD]) years for males and 40±7 years for females, obviously reflecting the milder phenotype in female patients.[3] Among cardiologists, Danon disease is now being increasingly recognized as a cause of hypertrophic cardiomyopathy especially in children.[5–7]

Skeletal myopathy, usually mild, is present in most male patients (90%), but only in a minority of female patients (33%).[3] Patients do not lose the ability to walk despite the myopathy. Weakness and atrophy predominantly affect shoulder-girdle and neck muscles, but distal muscles can also be involved. Interestingly, all male patients show serum CK levels 5- to 10-fold above the upper limits of normal, even in the preclinical state. Therefore, Danon disease should be considered in the differential diagnosis of boys with cardiomyopathy and high serum CK. In contrast, serum CK is elevated in only 63% of female patients. In women, therefore, normal CK does not rule out the diagnosis of Danon disease. Other muscle enzymes including serum aspartate aminotransferase (AST), alanine aminotransferase (ALT), and lactate dehydrogenase (LDH) are also increased. Electrophysiologically, myopathic units have been seen in all male patients studied. In addition, myotonic discharges were recorded in three of 10 male patients.[3]

Although both original patients reported by Danon and colleagues had mental retardation, this manifestation is mild and is absent in 30% of male patients. In the authors' study, there has been only one female patient with mental retardation (1/18, 6%).[3] Brain magnetic resonance imaging (MRI) is usually normal. In two autopsy cases, the authors found vacuolar changes in the cytoplasm of the red nucleus.[8] More recently, the authors' group reported lysosomal storage and advanced senescence in the brain of a Danon disease patient.[9] However, it is still unknown whether or not these abnormalities directly account for the mental retardation.

So far, variable clinical complications have been known in Danon disease. Hepatomegaly was noted in 36% of male patients and splenomegaly was seen in 5% in the authors' study.[3] Ophthalmic abnormalities including retinopathy and cone–rod retinal dystrophy were also reported.[10–12] Retinal impairments have potentially progressive decrease of visual acuity. Foot deformity was sometimes noticed. Nerve conduction studies were usually normal, but sensory and motor neuropathy with pes cavus was rarely reported.[13] Unusually, autism was presented in male children with Danon disease.[14] Cerebrovascular complications have previously been reported.[15] Embolic complications may be relatively common in patients with Danon disease, and early recognition of cardiac arrhythmia and anticoagulant therapy might prevent death or disability because of cerebrovascular events. Restrictive lung problems, possibly related to respiratory muscle weakness, were reported in a few male patients.[16] Clinical features of Danon disease may be broader than previously thought.

In LAMP-2 knockout mice, a wider variety of organs is affected, including liver, kidney, pancreas, small intestine, thymus, and spleen, in addition to heart and skeletal muscle.[17] Similarly, autopsy study showed vacuolar changes in a wide variety of tissues, including cardiac, skeletal, and smooth muscles, and liver.[8] Therefore, Danon disease in mice is essentially a systemic disorder.[18]

Muscle Pathology

Muscle pathology provides an important clue for the diagnosis. As discussed below, the genetic test is now available and can be performed instead of a muscle biopsy; however, considering the rarity of the disease and the absence of a mutation hotspot, it is not cost-effective to screen patients for a mutation in *LAMP-2* without a prior biopsy demonstrating vacuolar myopathy.

In muscle biopsies of Danon disease patients, variation of fiber size is mild to moderate and necrotic fibers are usually not seen. Muscle samples show many scattered intracytoplasmic vacuoles, which, on hematoxylin and eosin staining, often look like solid basophilic granules. These vacuoles are so tiny that they can easily be overlooked (Figure 37.1). Interestingly, the vacuolar membranes have acetylcholinesterase activity and are highlighted by histochemical stains for acetylcholinesterase (Figure 37.1) and nonspecific esterase.[3,19–21] Acetylcholinesterase is present at the neuromuscular junction in specialized sarcolemmal areas called junctional folds. Therefore, the presence of acetylcholinesterase activity indicates that the vacuolar membrane has features of sarcolemma. This characteristic has been confirmed by the immunohistochemical demonstration of other sarcolemma-specific proteins.[21] In fact, virtually all sarcolemmal proteins are